NASA TECHNICAL NOTE

NASA TN D-2794

THE VACUUM ULTRAVIOLET RADIATION FROM N^+- AND O^+-ELECTRON RECOMBINATION IN HIGH-TEMPERATURE AIR

by Gerhard E. Hahne

Ames Research Center

Moffett Field, Calif.

NATIONAL AERONAUTICS AND SPACE ADMINISTRATION • WASHINGTON, D. C. • JUNE 1965

NASA TN D-2794

THE VACUUM ULTRAVIOLET RADIATION FROM N^+- AND O^+-ELECTRON RECOMBINATION IN HIGH-TEMPERATURE AIR

By Gerhard E. Hahne

Ames Research Center
Moffett Field, Calif.

NATIONAL AERONAUTICS AND SPACE ADMINISTRATION

For sale by the Clearinghouse for Federal Scientific and Technical Information
Springfield, Virginia 22151 – Price $3.00

THE VACUUM ULTRAVIOLET RADIATION FROM N^+- AND O^+-ELECTRON RECOMBINATION IN HIGH-TEMPERATURE AIR

By Gerhard E. Hahne
Ames Research Center

SUMMARY

A free electron may, while interacting with an N^+ or an O^+ ion, fall into the 2p shell to form a bound state of a neutral N or a neutral O atom, respectively, the transition being accompanied by the emission of a quantum of light. If the N^+ or O^+ ion is initially in a state of its ground configuration, for allowed transitions, this light will be of wavelength $\lambda \leq 1130$ Å for nitrogen, and $\lambda \leq 911$ Å for oxygen (i.e., in the region of vacuum ultraviolet wavelengths).

The first step in estimating the contribution of such transitions to the rate of radiation of heated air was to calculate the cross sections for the inverse, photoionization processes, using the general formula of Burgess and Seaton. Given the composition of a sample of air, its absorption coefficient can be calculated from these photoionization cross sections, and if local thermodynamic equilibrium is assumed, the rate of radiation of air due to the corresponding recombination processes follows from Kirchhoff's law. This rate of radiation, integrated over the wavelength region from 400 Å to 1130 Å, has been calculated for air at several temperatures between 8,000° K and 24,000° K and several densities between 10^{-6} and 10^2 standard atmospheres for each temperature.

In addition, data have been tabulated to facilitate calculation of the intensity (integrated over wavelength) of vacuum ultraviolet wavelength light at the surface of uniform (constant temperature and density) "thick" bodies of heated air.

INTRODUCTION

Photorecombination of low-energy electrons with singly charged nitrogen or oxygen ions into low-lying states of the corresponding neutral atoms will give rise to light in the vacuum ultraviolet wavelength region. The range of temperatures and densities taken by the hot-gas cap forward of a blunt vehicle, moving into the earth's atmosphere at speeds of the order of escape speed, is such that these atoms and ions may dominate the population of species present there. Should this be the case, and depending on the cross sections for the above-mentioned recombination processes, large amounts of vacuum ultraviolet light may be emitted by the air in the gas cap, thereby imposing a significant heating load on the vehicle.

Calculations of the air radiation arising from this source have been carried out by Nardone, Breene, Zeldin, and Riethof (ref. 1), and by Sewell (ref. 2). The predictions in these two works are not in close agreement; the former work shows radiation rates sometimes six times larger, despite the fact that Sewell has also included the relatively long wavelength light emitted in photorecombination of electrons into some higher excited states of nitrogen and oxygen.

In view of both the above-mentioned discrepancies and the development by Burgess and Seaton (ref. 3) of a semiempirical formula which enables the rapid calculation of approximate atomic photoionization cross sections, further study of this problem seemed not only desirable but capable of yielding plausible results with modest effort.

The present investigation was undertaken, then, to carry out the following tasks: first, using, in particular, the formula of Burgess and Seaton, to calculate the cross sections for photoionization of nitrogen and oxygen atoms from certain low-lying quantum states; second, to apply these photoionization cross sections to the calculation of the rate of radiation of air due to the inverse, recombination processes; third, to compare the results obtained with the corresponding results of other authors and to discuss the underlying methods used in the several calculations.

SYMBOLS

$a_o = \hbar^2/me^2$	first Bohr radius of the (infinite nuclear mass) hydrogen atom
$B(\lambda_1,\lambda_2)$	integral of B_λ re λ over the wavelength range $\lambda_1 \leq \lambda \leq \lambda_2$
$B_\lambda, B_\lambda(T)$	Planck black body distribution of light energy flux
C_l	dimensionless constants, depending on terms of initial atom and final ion, etc., which arise in the calculation of atomic photoionization cross sections from central field wave functions
c	speed of light
E	energy parameter[1] in a radial Schrödinger equation
e	absolute value of the charge on the electron; base of Naperian logarithms
F(r,E)	function (bound state or continuum type) satisfying a radial Schrödinger equation in which the energy parameter is E

[1]These energies will be given as dimensionless multiples of the Rydberg unit, one unit being $me^4/2\hbar^2$, or about 13.605 electron volts.

$f(L/L_o)$	$I(\lambda_1,\lambda_2,L)/B(\lambda_1,\lambda_2)$ where T and ρ are given and fixed
$G_{k\ell}, G_{k\ell}(r)$	continuum one-electron radial wave function
h	Planck's constant
$\hbar$	$h/2\pi$
$I_{n\ell}$	threshold energy[1] for ionization of an atom by removal of an $n\ell$ shell electron
$I_\lambda, I_\lambda(L)$	spectral distribution of light energy flux; monochromatic intensity
$I(\lambda_1,\lambda_2;L)$	integral of $I_\lambda(L)$ over the wavelength range $\lambda_1 \leq \lambda \leq \lambda_2$
J	$J(\lambda_1,\lambda_2)$ if λ_1 and λ_2 are given and fixed
J_λ	monochromatic emission coefficient, or spectral radiance, of a sample of gas
$J(\lambda_1,\lambda_2)$	integral of J_λ re λ over the wavelength range $\lambda_1 \leq \lambda \leq \lambda_2$
k	Boltzmann's constant; absolute value of the square root of the kinetic energy[1] of a free electron
k_λ	absorption coefficient of a gas at wavelength λ
k_λ'	absorption coefficient corrected for stimulated emission
$\bar{k}(\lambda_1,\lambda_2)$	mean absorption coefficient in the wavelength range $\lambda_1 \leq \lambda \leq \lambda_2$; $k(0,\infty)$ = Planck mean absorption coefficient
L	length of a light path
L_o	$1/\bar{k}(\lambda_1,\lambda_2)$ where $T,\rho,\lambda_1,\lambda_2$ are given and fixed
l, l'	distance along a light path; one-electron angular momentum quantum numbers
m	electron mass
N	number of electrons in an atom or ion
$N_{n\ell}$	normalization constant for a bound state radial wave function
n	principal quantum number (integer, ≥ 1)
n*	effective principal quantum number (real, > 0)
$O(x)$	loosely speaking, a term of the order of x where x is real, > 0

[1]See footnote 1, page 2.

$P_{n\ell}, P_{n\ell}(r)$	bound state radial wave function
r	distance, in dimensionless multiples of a_o, from the nucleus of an atom
r_o	effective radius of the core of an atom or ion
T	absolute temperature
$V(r)$	effective potential energy[1] function
Z	atomic number of a nucleus
$\alpha = e^2/\hbar c$	Sommerfeld's fine structure constant; also used as L/L_o
$\Gamma(z)$	the gamma function of the complex number z
Δ	weighted mean square fluctuation of the absorption coefficient
$\delta_\ell, \delta_\ell(k^2)$	phase shift
ϵ, ϵ'	energy[1] parameter for a one-electron quantum state; related to E and ζ by $\epsilon = E/\zeta^2$
ζ	$Z - N + 1$ for an atom or ion with atomic number Z and N electrons
λ	wavelength of a quantum of light
μ	quantum defect
ρ	air density
ρ_o	standard density of air, 1.225×10^{-3} g cm^{-3}
σ	cross section

THEORY

Processes

The recombination (and corresponding photoionization) processes treated in the present work are those for which there is initially (or finally) a free electron in the presence of a singly charged nitrogen or oxygen ion in one of the states of its ground configuration, and for which the final (initial) state consists of a neutral nitrogen or oxygen atom in a state belonging to its ground configuration, plus a photon. Since fine structure effects are small, these transitions are conveniently grouped according to the total orbital and spin angular momenta of the ion and atom; there will be six groups of allowed transitions (in the dipole approximation) for each of the two atoms. In nitrogen these are:

[1]See footnote 1, page 2.

(a) $1s^2 2s^2 2p^2(^3P)$ + free electron $\longleftrightarrow$ $1s^2 2s^2 2p^3(^4S^o)$ + photon

(b) $1s^2 2s^2 2p^2(^3P)$ + free electron $\longleftrightarrow$ $1s^2 2s^2 2p^3(^2D^o)$ + photon

(c) $1s^2 2s^2 2p^2(^1D)$ + free electron $\longleftrightarrow$ $1s^2 2s^2 2p^3(^2D^o)$ + photon

(d) $1s^2 2s^2 2p^2(^3P)$ + free electron $\longleftrightarrow$ $1s^2 2s^2 2p^3(^2P^o)$ + photon

(e) $1s^2 2s^2 2p^2(^1D)$ + free electron $\longleftrightarrow$ $1s^2 2s^2 2p^3(^2P^o)$ + photon

(f) $1s^2 2s^2 2p^2(^1S)$ + free electron $\longleftrightarrow$ $1s^2 2s^2 2p^3(^2P^o)$ + photon

The longest photon wavelengths for which the above can occur are called the threshold wavelengths. For the above transitions, the threshold wavelengths are: (a) 852 Å, (b) 1020 Å, (c) 883 Å, (d) 1130 Å, (e) 964 Å, (f) 826 Å.

In oxygen, the transitions are:

(a) $1s^2 2s^2 2p^3(^4S^o)$ + free electron $\longleftrightarrow$ $1s^2 2s^2 2p^4(^3P)$ + photon

(b) $1s^2 2s^2 2p^3(^2D^o)$ + free electron $\longleftrightarrow$ $1s^2 2s^2 2p^4(^3P)$ + photon

(c) $1s^2 2s^2 2p^3(^2P^o)$ + free electron $\longleftrightarrow$ $1s^2 2s^2 2p^4(^3P)$ + photon

(d) $1s^2 2s^2 2p^3(^2D^o)$ + free electron $\longleftrightarrow$ $1s^2 2s^2 2p^4(^1D)$ + photon

(e) $1s^2 2s^2 2p^3(^2P^o)$ + free electron $\longleftrightarrow$ $1s^2 2s^2 2p^4(^1D)$ + photon

(f) $1s^2 2s^2 2p^3(^2P^o)$ + free electron $\longleftrightarrow$ $1s^2 2s^2 2p^4(^1S)$ + photon

The corresponding threshold wavelengths in oxygen are: (a) 911 Å, (b) 732 Å, (c) 666 Å, (d) 828 Å, (e) 744 Å, (f) 858 Å.

The above wavelength thresholds have been calculated from data in reference 4. The energy of a term was taken to be the center of gravity[2] of its fine structure levels.

One of the selection rules for dipole transitions requires that $\Delta l = \pm 1$ for the jumping electron, so that the free electron wave functions will be either s wave or d wave, for the above transitions.

General

Milne's formula (refs. 5 and 6) relates the cross section for radiative recombination of a free electron and positive ion into a state of the

---

[2]The center of gravity of a set of n levels with energies E_i and statistical weights g_i, $i = 1, 2, \ldots, n$, is defined as $\sum_{i=1}^{n} g_i E_i \Big/ \sum_{i=1}^{n} g_i$.

resulting atom to the cross section for the reverse, photoionization process. The latter cross section is more convenient to work with since it has a finite discontinuity at the threshold.

In the central field approximation for the wave function of an atom or ion, the cross section for absorption of a photon of energy $I_{n\ell} + k^2$, together with excitation of an electron from an $n\ell$ shell to the continuum, can be expressed in terms of one-electron radial wave functions as follows (ref. 3):

$$\sigma = \frac{4\pi\alpha}{3} a_o^2 (I_{n\ell} + k^2) \sum_{\ell' = \ell \pm 1} C_{\ell'} \left| \int_o^\infty P_{n\ell}(r) r G_{k\ell'}(r) dr \right|^2 \tag{1}$$

where σ is the total photoionization cross section; $I_{n\ell}$ and k^2, both in Rydbergs, are the threshold energy for ejection of the $n\ell$ shell electron, and kinetic energy of the ejected electron, respectively; the $C_{\ell'}$ are certain coefficients that depend on ℓ, ℓ' and the states of the initial atom and residual ion (see ref. 3); $P_{n\ell}(r)$ is the radial wave function of an $n\ell$ shell electron, satisfying

$$P_{n\ell}(0) = P_{n\ell}(\infty) = 0 \tag{2a}$$

and

$$\int_o^\infty P_{n\ell}^2(r) dr = 1 \tag{2b}$$

The functions $G_{k\ell'}(r)$, with $\ell' = \ell \pm 1$, are continuum radial wave functions for the free electron in the field of the ion core, satisfying

$$G_{k\ell'}(0) = 0 \tag{3}$$

and are normalized by requiring their asymptotic amplitude for large r to be $k^{-1/2}$.

Both $P_{n\ell}$ and $G_{k\ell'}$ satisfy a radial Schrödinger equation of the type (omitting exchange terms)

$$\frac{d^2}{dr^2} F_\ell(r,E) + \left[E - V(r) - \frac{\ell(\ell+1)}{r^2} \right] F_\ell(r,E) = 0 \tag{4}$$

where for the continuum functions $E = k^2$ is the free electron's kinetic energy; for bound states E will be negative, and is chosen so that the boundary conditions (2a) can be satisfied. The quantity $V(r)$ is an effective potential energy function for the jumping electron, and may be different for different states of the core and jumping electron; $V(r)$ must have the asymptotic form of a Coulomb potential for large r:

$$V(r) \xrightarrow[r \to \infty]{} -\frac{2\zeta}{r} \tag{5}$$

where for an atom with a nuclear charge of Z units, and a total of N electrons, $\zeta = Z - N + 1$. Therefore, the asymptotic forms of the radial wave functions in the continuum are (ref. 7)

$$G_{k\ell'}(r) \xrightarrow[r \to \infty]{} \frac{\sin\left[kr + \frac{\zeta}{k} \log 2kr - \frac{\ell'\pi}{2} + \arg \Gamma\left(\ell' + 1 - i\frac{\zeta}{k}\right) + \delta_{\ell'}\left(\frac{k^2}{\zeta^2}\right)\right]}{\sqrt{k}} \tag{6}$$

where $\delta_{\ell'}(k^2/\zeta^2)$ is a phase shift which would be identically zero if $V(r)$ were an exact Coulomb potential function. For the bound state functions (ref. 8)

$$P_{n\ell}(r) \xrightarrow[r \to \infty]{} N_{n\ell} r^{n^*} e^{-r/n^*} \tag{7}$$

where $N_{n\ell}$ is a normalization constant which is determined by condition (2b), and n^*, an effective principal quantum number, is determined from the eigenvalue E (of the radial Schrödinger equation satisfied by $P_{n\ell}$) by the following formula:

$$n^* = \frac{\zeta}{\sqrt{-E}} \tag{8}$$

We note that the quantum defect μ for a level with principal quantum number n is defined as follows:

$$\mu = n - n^* \tag{9}$$

where μ depends on n and ℓ, and will be zero for the states of hydrogen-like atoms. The quantum defects for a series of levels in an atom will often be found to lie on a smooth curve if plotted as a function of energy E, and will tend to a finite limit as $n \to \infty$ (see refs. 7 and 9 for details and examples).

The Coulomb Approximation

Now it is generally a difficult task to obtain a reasonably accurate potential energy function $V(r)$ for a given $n\ell$ shell wave function in a given atom or ion. Moreover, it has been found (refs. 3 and 8) that for a wide class of radiative transitions, the principal contributions to the dipole length integrals in equation (1) come from r large enough that $V(r)$ has essentially reached its asymptotic Coulomb form. Therefore, except as it indirectly influences the behavior of the radial wave functions for large r, the detailed behavior of $V(r)$ for small r may be unimportant.

Given the quantum number ℓ, only two quantities are needed to determine a bound state radial wave function in this region (i.e., the region for which r is so large that eq. (5) holds), the normalization constant $N_{n\ell}$, and the energy parameter E. For a continuum state radial wave function, ℓ' and the wave number k are given, and only the phase shift $\delta_{\ell'}(k^2/\zeta^2)$ is needed.

Once these quantities are known for the states of interest, the integrals in equation (1) can be approximated by neglecting the contributions for r less than the radius r_o at which the potential energy $V(r)$ begins to depart significantly from its asymptotic form. This approximation is known as the Coulomb approximation.

All this would be of little practical interest, however, if it were not for the fact that all of the determining quantities for the asymptotic forms of the radial wave functions may be inferred from empirical data on atomic energy levels. A means of doing so for bound state wave functions was given by Bates and Damgaard (ref. 8) as a part of their development of the Coulomb approximation for bound-bound transitions (see also ref. 10). Subsequently, Seaton (ref. 7) showed that the Bates-Damgaard formula for normalizing bound radial wave functions was good only in the limit of large principal quantum number, and at the same time gave a more accurate formula. A method for determining bound-state energy parameters from empirical data which is somewhat more explicit than the Bates-Damgaard prescription is made plausible in appendix A of the present work.

For free-electron wave functions Seaton (refs. 7, 11, and 12), using the theory of the quantum defect method developed in a different context by Ham (ref. 13) and others, showed that the phase shifts for continuum functions could be obtained by extrapolation to positive energies of π times the quantum defect[3] for the corresponding bound state functions. Subsequently, Burgess and Seaton (refs. 3 and 16) developed a general formula for calculating bound-free transition integrals in the Coulomb approximation; their results were used in the present calculation, and are outlined below.

Burgess and Seaton define the quantities $g(n^*l;\epsilon' l')$ in terms of the radial matrix elements as follows:

$$g(n^*l;\epsilon' l') = I_{nl} \int_o^\infty P_{nl}(r) r G_{k l'}(r) dr \tag{10}$$

$n^* = \zeta/\sqrt{I_{nl}}$ is the effective principal quantum number of the initial state wave function, I_{nl} is the threshold energy for the photoionization process in question, and $k^2 = \epsilon'\zeta^2$ is the kinetic energy of the final state free electron. We note that $g(n^*l;\epsilon' l')$ has no explicit ζ dependence. Formula (1) for the cross section becomes

$$\sigma = \frac{4\pi\alpha}{3} a_o^2 \frac{I_{nl} + k^2}{I_{nl}^2} \sum_{l'=l\pm 1} C_{l'} \left| g(n^*l;\epsilon' l') \right|^2 \tag{11}$$

---

[3]This is valid only for small positive energies, such that $2\pi\zeta/k \gg 1$; Seaton (ref. 7) gives a more elaborate formula connecting $\mu'(\epsilon')$ and $\delta'(\epsilon')$, where $\epsilon' = k^2/\zeta^2$, for the general case. See also Moiseiwitsch (ref. 14) and Norman (ref. 15).

Burgess and Seaton give the following interpolation formula for the $g(n^*l;\epsilon' l')$:

$$g(n^*l;\epsilon' l') = \frac{G(n^*l;\epsilon' l')}{\rho^{1/2}(n^*,l)} \cos \pi[n^* + \mu'(\epsilon') + \chi(n^*l;\epsilon' l')] \tag{12}$$

$$G(n^*l;\epsilon' l') = (-1)^{l+1} G_{ll'}(n^*)(1 + \epsilon' n^{*2})^{-\gamma_{ll'}(n^*)} \tag{13}$$

$$\chi(n^*l;\epsilon' l') = \chi_{ll'}(n^*) + \frac{\epsilon' n^*}{1 + \epsilon' n^*} \alpha_{ll'} + \frac{\epsilon' n^{*2}}{1 + \epsilon' n^{*2}} \beta_{ll'}(n^*) \tag{14}$$

where $\mu'(\epsilon')$ is the extrapolated quantum defect of the $n'l'$ series. The quantities $G_{ll'}(n^*)$, $\gamma_{ll'}(n^*)$, $\alpha_{ll'}$, $\beta_{ll'}(n^*)$, $\chi_{ll'}(n^*)$ are tabulated in reference 3, and

$$\rho(n^*,l) = 1 + \frac{2}{n^{*3}} \frac{\partial \mu(\epsilon)}{\partial \epsilon} \tag{15}$$

in equation (15), $\mu(\epsilon)$ is the interpolated quantum defect for the nl series, and the derivative is evaluated at

$$\epsilon = -\frac{1}{n^{*2}} = -\frac{I_{nl}}{\zeta^2} \tag{16}$$

I_{nl} being the absolute value of the energy of the jumping electron in its initial bound state, or, what is the same, the threshold energy of the photoionization process considered (see appendix A).

The energy levels from which the ϵ and n^* values were calculated[4] were taken from Moore (ref. 4); the values of

$$C_{l'}, \quad G_{ll'}(n^*)/(n^* - 1)^{1/2}, \quad \gamma_{ll'}(n^*), \quad \chi_{ll'}(n^*), \quad \alpha_{ll'}, \quad \beta_{ll'}(n^*)$$

were obtained from tables II, VII, and VIII of reference 3, by graphical interpolation or extrapolation of that data if necessary; the values of $\rho^{1/2}(n^*,l)/(n^* - 1)^{1/2}$ were calculated using the following formula, given in reference 7, and proved in reference 17:

$$\rho(n^*,l) = \frac{(n^* - 1)(n^* + 2)}{n^*(n^* + 1)} \tag{17}$$

This is a good approximation for $\rho(n^*,l)$ if n^* is close to 1 for a 2p wave function.

[4] Fine structure splittings were neglected; the energy of a term was taken to be its center of gravity.

In obtaining the values of the parameters in the Burgess-Seaton formulas from the tables in reference 3, it is sometimes necessary to extrapolate functions of the effective principal quantum number n^* which are tabulated only for somewhat widely spaced values of n^*. In particular, the cross sections calculated here are sensitive to the value taken for $G_{12}(n^*)$ for n^* close to 1.0, as obtained from table VIII in reference 3. We have assumed that the curve of the function $G_{12}(n^*)/(n^* - 1)^{1/2}$ has zero slope at $n^* = 1.00$.

The lack of knowledge of a sufficient number of atomic energy levels prevents reliable extrapolation from being made for many series in NI and OI; this is true, in particular, for series in which the ionic core is not in a state of the lowest term of its ground configuration. As a rough approximation for these cases, the quantum defects have been chosen to be 0.0 for d functions, 1.0 for s functions. The effect of any errors thereby incurred is mitigated by the fact that these N^+- or O^+-electron recombination processes, in which the ion is not initially in its ground term, give rise to relatively small contributions to air radiation; in turn, this is due to the low populations of the excited core states for all but the highest temperatures considered here.

For the series in NI in which the core structure is $1s^2 2s^2 2p^2(^3P)$, and series in OI in which the core is $1s^2 2s^2 2p^3(^4S^o)$, many of the energy levels, where the outer electron is ns or nd, are tabulated in reference 4, volume I, with additions and corrections in volumes II and III. Also, Kvifte (ref. 18), and Eriksson and Isberg (ref. 19) have given new or revised energies for some levels of the series $2p^3(^4S^o)$ ns and $2p^3(^4S^o)$ nd in OI; new or revised energies for a number of levels in NI can be found in Eriksson (ref. 20) and Eriksson and Johansson (ref. 21).

For OI the calculation and extrapolation of the quantum defects is relatively straightforward since the $^4S^o$ core has no fine structure. The quantum defects used in the present calculation were (ref. 19):

For the series $1s^2 2s^2 2p^3(^4S^o)$ ns $^3S^o$

$$\mu'(\epsilon') = 1.1499417 - 0.0816399\epsilon' + 0.047241\epsilon'^2 + 0.043095\epsilon'^3 \qquad (18a)$$

For the series $1s^2 2s^2 2p^3(^4S^o)$ nd $^3D^o$

$$\mu'(\epsilon') = 0.0242064 + 0.050812\epsilon' + 0.01301\epsilon'^2 - 0.000011576(\epsilon' + 0.079224)^{-1} \qquad (18b)$$

For NI the situation is less satisfactory. Here there are three closely spaced series limits as a result of the fine structure of the ^3P core, and, correspondingly, there are serious departures from LS coupling for high series members (ref. 9). It is particularly important to have good energy values for the levels of the $2p^2(^3P)$ nd series since it turns out that the probability of a radiative transition from a 2p to a continuum d state is usually somewhat greater than from a 2p to a continuum s state

for the processes considered here. There are some gaps and uncertainties in the series levels which are given by Moore (ref. 4, vol. I), and the term values of ns and nd series are given in references 20 and 21 for levels of the $2p^2(^3P)$ 3d, 3s, 4s, and 5s configurations only. In the absence of data which would allow a more refined treatment, the method decided upon was to extrapolate the quantum defect of the center of gravity of all the levels of $2p^2(^3P)$ ns or nd. The threshold energy for ionization was considered to be the center of gravity of the three series limits. The quantum defects calculated in this manner were found to be reasonable only for the lower series members, for which the various level splittings are small compared to the binding energy for the $n\ell$ electron. The extrapolated quantum defects obtained by representing the results for $n = 3$, 4, and 5 by a straight line were:

For the series $1s^2 2s^2 2p^2(^3P)$ ns

$$\mu'(\epsilon') = 1.13 - 0.10\epsilon' \tag{19a}$$

and for the series $1s^2 2s^2 2p^2(^3P)$ nd

$$\mu'(\epsilon') = 0.037 \tag{19b}$$

These formulas for quantum defects of nitrogen series, and those for series in oxygen, are probably valid at best for $\epsilon' \leq 0.5$, a condition about as restrictive as the condition $\exp(-2\pi/\sqrt{\epsilon'}) \ll 1$, which limits the validity of the extrapolation of π times the quantum defects into the continuum phase shifts (ref. 7). The photoionization cross sections for N and O, calculated using these quantum defects, are, therefore, likely to be in error for k^2/ζ^2 of the order of, or greater than, 1. These errors will not be important at the lower of the temperatures considered here since most of the corresponding recombination light from air will come from recombination of ions with low energy free electrons, so that it is sufficient to have accurate knowledge of the photoionization cross sections near threshold only. For the higher temperatures, our results will be less reliable.

We are now in a position to calculate approximate photoionization cross sections for all the processes in nitrogen and oxygen to be considered in the present work. Once the concentrations in air of the relevant species are known as a function of temperature and density, we will be prepared to use these cross sections for the calculation of macroscopic radiative quantities. These subjects are considered in the following two sections.

Populations

Among the sets of data on the composition of air known to us, the graphs given in the work of Sewell, et al. (ref. 22) give compositions for the widest range of densities ($10^{-6} \leq \rho/\rho_o \leq 10^2$) and finest mesh of temperatures in the region of interest here, and we have consequently used reference 22 as the exclusive source of these data.

It turns out (see next section "Radiative Transfer") that for the purpose of the present calculation, it is sufficient to know, as a function of air temperature and density, first the number densities of neutral nitrogen and oxygen atoms, and second, the fraction of nitrogen atoms which are in states of each of the three terms ($^4S^o$,$^2D^o$,$^2P^o$) of the ground configuration of nitrogen ($1s^2 2s^2 2p^3$), and the fraction of oxygen atoms which are in states of each of the three terms (^3P,^1D,^1S) of the oxygen ground configuration ($1s^2 2s^2 2p^4$). The first of these sets of data can be calculated directly from the molar concentrations given in reference 22, but fractional populations were not given there, nor was there given an explicit prescription for calculating the atomic partition functions. However, it was implied that a fixed, finite number of states were used to calculate the partition functions, and we have verified this by calculating the equilibrium constants in the Saha equation (see, e.g., ref. 23) for the reactions $N \rightleftarrows N^+ + e^-$, $O \rightleftarrows O^+ + e^-$ from the composition data in reference 22 and observing that these equilibrium constants did not vary significantly as a function of density, for fixed temperature (there were often unsystematic variations of a few percent, resulting in part from uncertainties in reading values from the graphs, and in part from unknown causes).

The atomic energy levels used to calculate partition functions in reference 22 were taken from Moore (ref. 4). Since the partition function either for N^+ or for O^+ is relatively insensitive, at temperatures $T < 25{,}000^o$ K, to the criterion for truncating the respective sum over states, it is possible to work backward from the Saha equation and deduce the partition function, and hence the truncation criterion, for either N or O. It was found that the partition functions for both N and O were calculated, in reference 22, by including all states whose energies were less than roughly 105,500 cm^{-1} above the respective ground states. (It is seen from the tables of Moore (ref. 4), that this energy is just greater than that of $1s^2 2s^2 2p^2(^3P)$ 3d $^2D_{5/2}$ in nitrogen and $1s^2 2s^2 2p^3(^4S^o)$ 5d $^3D^o_{3,2,1}$ in oxygen.) These partition functions were used to calculate the needed fractional level populations.

We note that as far as reference 22 and this paper are concerned, cold air consists of 78.0881 percent N_2, 20.9795 percent O_2, and 0.9324 percent Ar (these are mole percentages), and the standard state of air is that for which the pressure is 1 atmosphere (= 1.01325×10^6 dyne cm^{-2}), and the temperature is 288.16^o K, so that $\rho_o = 1.225 \times 10^{-3}$ g cm^{-3}.

Radiative Transfer

In order to present the results of this study in usable form they will be expressed in terms of macroscopic radiative quantities which arise in the context of a radiation flow problem which we now briefly present and discuss.[5]

The radiative transfer problem which we will solve consists in finding the flux of radiant energy emitted at any given point on the surface of a body

[5]Much of this theory is developed in more detail in the texts of Unsöld (ref. 24) and of Chandrasekhar (ref. 25).

of gas, and in any given direction through the point on the surface. The gas will be assumed (1) to have local temperature and composition which do not vary in time or within the spatial limits of the body, (2) to be isotropic in its interaction with radiation, and (3) to interact with radiation only in the form of processes of simple absorption and spontaneous or stimulated emission (scattering will be neglected). The emission and absorption of radiation will be assumed not to perturb the state of temperature or composition of the gas significantly. Finally, the radiation flow field will be assumed to have zero inward flux at the surface of the gas body.

We remark that these assumptions imply that any radiation present in the system will be unpolarized. The assumption of zero inward flux at the surface of the body requires that the body be convex (i.e., the straight line segment connecting any pair of points in the body must lie entirely within the body).

The probability per unit length of absorption of a photon of wavelength λ in the gas is k_λ, where

$$k_\lambda = \sum_{s,\alpha} n_{s\alpha}\sigma_{s\alpha}(\lambda) \tag{20}$$

The sum ranges over the states (α) of each species (s) in the gas; $n_{s\alpha}$ is the number density of, and $\sigma_{s\alpha}$ is the photon absorption cross section for, particles of species s, in state α.

We let I_λ be the monochromatic intensity of radiation flux at a given point, and in a given direction through the point, the dimensions of I_λ being $(\text{energy})(\text{area})^{-1}(\text{time})^{-1}(\text{solid angle})^{-1}(\text{wavelength})^{-1}$. The monochromatic emission coefficient at a point of the gas, and in a given direction from the point, J_λ, has the dimensions $(\text{energy})(\text{volume})^{-1}(\text{time})^{-1}(\text{solid angle})^{-1}(\text{wavelength})^{-1}$.

In the system being considered, the radiation flow is such that the equation of radiative transfer may be written in terms of the flux $I_\lambda(l)$ of radiation along any given directed line, where l is a measure of distance from some fixed point on the line. The situation is illustrated in sketch (a).

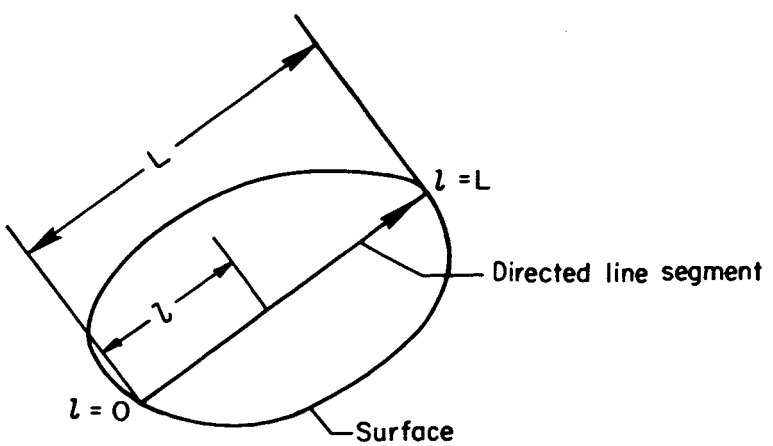

Sketch (a)

The equation of radiative transfer along the directed line segment within the body is (ref. 23, p. 98; ref. 24, p. 107; ref. 25, p. 12):

$$\frac{dI_\lambda(l)}{dl} = -k_\lambda' I_\lambda(l) + J_\lambda \tag{21}$$

where k_λ' is the absorption coefficient corrected for stimulated emission, J_λ is the monochromatic emission coefficient (neither k_λ' nor J_λ depends on position or direction within the gas body), and I_λ is the flux of radiation at a point l on the line segment and in the direction of the line segment.

On account of the assumption of thermodynamic equilibrium at temperature T in the gas, k_λ and k_λ' are related by

$$k_\lambda' = \left[1 - \exp\left(-\frac{hc}{\lambda kT}\right)\right] k_\lambda \tag{22}$$

and J_λ is given in terms of k_λ' and the Planck black body function $B_\lambda(T)$ according to Kirchhoff's law:

$$J_\lambda = k_\lambda' B_\lambda(T) \tag{23}$$

The quantity $B_\lambda(T)$ is of the same type as I_λ, and

$$B_\lambda(T) = \frac{2hc^2}{\lambda^5}\left[\exp\left(\frac{hc}{\lambda kT}\right) - 1\right]^{-1} \tag{24}$$

The equation of radiative transfer now becomes

$$\frac{dI_\lambda(l)}{dl} = -k_\lambda'[I_\lambda(l) - B_\lambda(T)] \tag{25}$$

If, as in sketch (a), we take $l = 0$ to be on the surface of the gas body and to be the tail end of the directed line segment, and $l = L$ to be on the surface and to be the head end of the line segment ($L \geq 0$ is called a diameter of the body, and is well defined on account of the body's convexity), the condition that no radiation enters the body at the surface implies that $I_\lambda(0) = 0$. The solution of equation (25) is, for this case,

$$I_\lambda(l) = B_\lambda(T)[1 - \exp(-k_\lambda' l)] \tag{26}$$

The flux of radiation leaving the body at the point of its surface corresponding to $l = L$ on the given line segment, and in the direction of the line segment, is $I_\lambda(L)$, where

$$I_\lambda(L) = B_\lambda(T)[1 - \exp(-k_\lambda' L)] \tag{27}$$

In the following discussion, since the temperature T will be uniform in the radiating media to be considered, we suppress the variable T.

It is easy to see from equation (27) that for a given wavelength λ, if $k_\lambda'L \gg 1$, $I_\lambda(L) \cong B_\lambda$; that is, this part of the radiation flux at the surface of the body approaches black body radiation. If, on the other hand, $k_\lambda'L \ll 1$, we have

$$I_\lambda(L) = k_\lambda'B_\lambda L + O[(k_\lambda'L)^2]B_\lambda \tag{28}$$

Should the condition $k_\lambda'L \ll 1$ hold for every diameter of the body (L being the length of a diameter), the gas body is said to be optically thin at wavelength λ. Using equation (28) an integration shows that the monochromatic rate of emission of light energy by the body as a whole will be, neglecting terms in $(k_\lambda'L)^2$,

$$\text{rate} = 4\pi V k_\lambda'B_\lambda = 4\pi V J_\lambda \tag{29}$$

where V is the volume of the body. This result is, of course, consistent with the definition of J_λ.

The relation $J_\lambda = k_\lambda'B_\lambda$ makes it possible to express the monochromatic emission coefficient, resulting from recombination of N^+ and O^+ ions with electrons in a body of air in thermal equilibrium, in terms of the concentrations of, respectively, N and O atoms. We will take advantage of this fact (in figs. 3 and 4) by giving the monochromatic emission coefficient per atom of nitrogen or of oxygen.

We have now developed the theory of radiative transfer to the point that we are able to calculate the monochromatic flux I_λ of light energy leaving a uniform (constant T and ρ) thick body of heated air at any given point of the surface of the body, and in any given direction. For some applications, it is sufficient to know only the integral over wavelengths of this flux. The remainder of this section is devoted to the introduction and relation of radiative quantities which arise in this context. Numerical values for some of these quantities are given in the graphs and tables as functions of air temperature and density, and, where applicable, as functions of the diameter L which a thick body of heated air may have in some given direction.

The Planck mean absorption coefficient is defined as follows:

$$\bar{k}_{\text{Planck}} = \frac{\int_0^\infty k_\lambda'B_\lambda \, d\lambda}{\int_0^\infty B_\lambda \, d\lambda} \tag{30}$$

In the present study, however, only a limited region of the wavelength spectrum will be considered, say $\lambda_1 \leq \lambda \leq \lambda_2$; a natural definition of the mean absorption coefficient for this case is

$$\bar{k}(\lambda_1,\lambda_2) = \frac{\int_{\lambda_1}^{\lambda_2} k_\lambda' B_\lambda \, d\lambda}{\int_{\lambda_1}^{\lambda_2} B_\lambda \, d\lambda} \tag{31}$$

We define other quantities accordingly:

$$B(\lambda_1,\lambda_2) = \int_{\lambda_1}^{\lambda_2} B_\lambda \, d\lambda \tag{32}$$

$$J(\lambda_1,\lambda_2) = \int_{\lambda_1}^{\lambda_2} J_\lambda \, d\lambda \tag{33}$$

$$I(\lambda_1,\lambda_2;L) = \int_{\lambda_1}^{\lambda_2} I_\lambda(L) d\lambda \tag{34}$$

For a gas body for which the conditions giving rise to equation (27) hold, and fixing λ_1 and λ_2, let

$$L_o = \frac{1}{\bar{k}(\lambda_1,\lambda_2)} \tag{35}$$

and

$$f\left(\frac{L}{L_o}\right) = \frac{I(\lambda_1,\lambda_2;L)}{B(\lambda_1,\lambda_2)} = \frac{\int_{\lambda_1}^{\lambda_2} (1 - e^{-k_\lambda' L}) B_\lambda \, d\lambda}{\int_{\lambda_1}^{\lambda_2} B_\lambda \, d\lambda} \tag{36}$$

The right-hand side of (36) can be expanded in power series in L:

$$f\left(\frac{L}{L_o}\right) = \frac{\int_{\lambda_1}^{\lambda_2} \left\{k_\lambda' L - \frac{1}{2} k_\lambda'^2 L^2 + O[(k_\lambda' L)^3]\right\} B_\lambda \, d\lambda}{B(\lambda_1,\lambda_2)} \tag{37}$$

From equations (31), (32), (34), (35), and (36) we find

$$f\left(\frac{L}{L_o}\right) = \frac{L}{L_o} - \frac{(1 + \Delta)}{2}\left(\frac{L}{L_o}\right)^2 + O\left[\left(\frac{L}{L_o}\right)^3\right] \tag{38}$$

where

$$\Delta = \frac{\int_{\lambda_1}^{\lambda_2} [k_\lambda' - \bar{k}(\lambda_1,\lambda_2)]^2 B_\lambda \, d\lambda}{\bar{k}(\lambda_1,\lambda_2)^2 B(\lambda_1,\lambda_2)} \tag{39}$$

The quantity Δ is non-negative, and is proportional to a weighted mean-square fluctuation of the absorption coefficient k_λ'. Its application is in the following context. Suppose we want to estimate the outgoing radiative flux at a point of the surface of a "thick" convex body of gas, supposed uniformly dense and hot, and in a direction along which the gas body has diameter L.

Substituting $\bar{k}(\lambda_1,\lambda_2)$ for k_λ' in equation (27), and using (32) and (34), we have the approximate formula

$$I(\lambda_1,\lambda_2;L) \cong [1 - e^{-\bar{k}(\lambda_1,\lambda_2)L}]B(\lambda_1,\lambda_2) \tag{40}$$

This formula will be useful only if Δ is sufficiently small.

In fact, if $\Delta > 0$, the estimate of $I(\lambda_1,\lambda_2;L)$ in formula (40) will be too large; that is,

$$[1 - e^{-\bar{k}(\lambda_1,\lambda_2)L}] \int_{\lambda_1}^{\lambda_2} B_\lambda \, d\lambda \geq \int_{\lambda_1}^{\lambda_2} (1 - e^{-k_\lambda' L}) B_\lambda \, d\lambda \tag{41}$$

The equality in (41) holds identically for all L if and only if $\Delta = 0$. If $\Delta \neq 0$, the equality holds in (41) if and only if $L = 0$. The proof of these results is given in appendix B.

We remark that the quantities Δ and $I(\lambda_1,\lambda_2;L)$ do not depend on the absorption coefficient k_λ' in any simple way. The values of these quantities given in the graphs and tables, therefore, will be of limited usefulness for air densities and temperatures for which processes other than those considered here (e.g., atomic line radiation, bremsstrahlung, and recombination of electrons with N^{++}, O^{++}, or N_2^+ ions) are important sources of radiation in the wavelength region 400 Å $\leq \lambda \leq$ 1130 Å.

Calculation

The numerical computation of the partition functions, cross sections, absorption coefficients, etc., was programmed for, and performed on, an electronic digital computer.

The effective principal quantum numbers and threshold energies for each photoionization channel were calculated from empirical atomic energy levels (ref. 4) according to the rules of appendix A. Equations (18a,b) and (19a,b), were used, where applicable, to calculate extrapolated quantum defects. Extrapolated quantum defects for other continuum levels were (in effect) put equal to zero. The phase shifts obtained from these quantum defects will be referred to in the discussion as the semiempirical phase shifts. The cross sections and derived quantities were calculated at intervals of 1 Å in the photon wavelength. Simpson's rule was used to calculate the quantities $B(\lambda_1,\lambda_2)$, $J(\lambda_1,\lambda_2)$, L_o, Δ, and $I(\lambda_1,\lambda_2;L)/B(\lambda_1,\lambda_2)$ for several values of L, with $\lambda_1 = 400$ Å, $\lambda_2 = 1{,}130$ Å, for 13 temperatures, $8{,}000^\circ \text{ K} \leq T \leq 24{,}000^\circ \text{ K}$, and 9 densities for each temperature, $10^{-6} \leq \rho/\rho_o \leq 10^2$.

The upper wavelength cutoff was taken to be 1,130 Å since none of the processes considered absorbs or emits light with $\lambda > 1{,}130$ Å. Because of the relative smallness of the Planck function $B_\lambda(T)$ for $T \leq 24{,}000^\circ$ K and $\lambda < 400$ Å, emission of radiation with $\lambda < 400$ Å was neglected throughout (in this connection, see figs. 3 and 4).

RESULTS AND DISCUSSION

Description of Graphs and Tables

The results of the calculation are presented according to the following scheme: (1) Figures 1 and 2 show the photoionization cross sections as a function of wavelength for six channels each in nitrogen and oxygen, and the labels on these curves correspond to those in the section "Processes"; (2) figures 3 and 4 show the monochromatic emission coefficient J_λ as a function of wavelength for an average atom of nitrogen or oxygen, respectively, for various temperatures;[6] (3) figure 5 shows the resulting integrated emission coefficient $J = J(\lambda_1,\lambda_2)$ of heated air as a function of temperature, for several densities, where $\lambda_1 = 400$ Å and $\lambda_2 = 1{,}130$ Å; (4) figure 6 shows the integral of the Planck function from 400 Å to 1,130 Å and from 0Å to ∞ as a function of temperature; (5) figure 7 compares, for representative cases of air temperature-density, the values of

$$I(400 \text{ Å}, 1{,}130 \text{ Å}; L)/B(400 \text{ Å}, 1{,}130 \text{ Å}) = f(L/L_o)$$

as a function of L/L_o, obtained according to the approximate formula given in equation (40), and according to the exact formula of equation (36); (6) figure 8 compares the photoionization cross sections for ground state nitrogen atoms as obtained from various theories and from experiment; (7) figure 9 compares the radiation from air ($\rho/\rho_o = 10^{-3}$), due to processes of N^+ and O^+ electron photorecombination, as calculated in references 1, 2, and the present work; (8) table I compares threshold photoionization cross sections calculated according to various theories; (9) table II gives the values of L_o, Δ, and

[6] In terms of these values and the composition data of ref. 22, J_λ for air is $n_N J_\lambda$ (nitrogen) + $n_O J_\lambda$ (oxygen), where n_N and n_O are the total number densities of nitrogen and oxygen atoms, respectively.

$I(400\ Å, 1{,}130\ Å; L)/B(400\ Å, 1{,}130\ Å)$ at a few values of L/L_o, for all of the air temperatures and densities treated.

Discussion of Photoionization Cross Sections

In order to determine the photoionization cross section of neutral nitrogen atoms, Ehler and Weissler (ref. 26) measured the absorption of light as it passed through a column of nitrogen excited by an electrical discharge. The measurement was done (1) with the discharge on, with light wavelengths ranging from 400 Å to 720 Å; (2) with the discharge off, but before the nitrogen atoms had recombined into molecules, at a wavelength of (in particular) 650 Å. The results of both versions of the experiment, along with the cross sections obtained by several theoretical calculations, are plotted in figure 8. In the second version of the experiment, where the presence of ions, or of nitrogen atoms in metastable states, was much less likely than in the first, the cross section was found to be 12.8×10^{-18} cm^2. In the following, we consider only the first version of the experiment.

There were two principal sources of uncertainty in the experimental results. The first was the estimation of the concentration of N_2, N_2^+, N, N^+, etc., in the discharge. On this point Ehler and Weissler implied that they believed the number which they used for the concentration of atomic nitrogen in the discharge was in error by, at most, a factor of 2, and was probably in error by considerably less than this. A relative error in the value taken for the concentration of atomic nitrogen would lead (roughly) to a similar relative error in the cross sections but in the opposite direction.

The second source of uncertainty was the random fluctuations of the measured values of intensity of light which had passed through the plasma. Here the fluctuations were such that the derived cross sections would all fall within the limits of the experimental cross sections shown on figure 8, plus or minus 4×10^{-18} cm^2 (i.e., if the species concentrations in the discharge are given and fixed at the values assumed by Ehler and Weissler).

All of the theoretical curves in figure 8 represent cross sections for the process photon plus $1s^2 2s^2 2p^3(^4S^o) \rightarrow 1s^2 2s^2 2p^2(^3P)$ plus free electron, in atomic nitrogen. The cross-section values of Nardone, et al., were inferred from their graph of the spectral radiance of the N^+ deionization continuum at 10,000° K (ref. 2, fig. 74). The values ascribed to the "modified" Kramers formula were calculated according to a method which to a certain extent accounts for the term structure of the nitrogen atom and ion. The modified and unmodified Kramers formulas are discussed in appendix C.

The cross sections (fig. 8) of Bates and Seaton were taken from the curve in reference 27. Since these values are in best agreement with the albeit uncertain experimental cross sections, we will consider in some detail the method of calculation used by Bates and Seaton. These authors obtained threshold cross sections for nitrogen by using Hartree-Fock type atomic wave functions in formula (1) of the present work. The 2p function was taken from Hartree and Hartree (ref. 28), and the zero-energy continuum functions were taken to be the numerically calculated (in ref. 27) s wave and d wave functions for an electron in the field of an O^+ ion. The threshold cross

section of 9.0×10^{-18} cm^2 represents the arithmetic mean of the values obtained by the dipole length formula (10.2×10^{-18} cm^2) and dipole velocity formula (7.7×10^{-18} cm^2). The cross-section values for photon energies above threshold were obtained by making use of earlier work of Bates (ref. 29), where an analytic formula for cross sections for photoionization of atoms by ejection of 1s, 2s, or 2p electrons was obtained. In reference 29, the continuum wave functions were taken to be hydrogen-like, and the bound state wave functions were taken to be analytic functions with variable parameters. Bates and Seaton chose the parameters in the analytic 2p type function to fit the nitrogen 2p function of Hartree and Hartree, and normalized the cross sections obtained (with Bates' formula of ref. 29) by a constant factor so as to be 9.0×10^{-18} cm^2 at threshold).

If Ehler and Weissler's empirical cross-section curve is assumed to have the correct shape (in particular that there is a maximum in the cross section at about 650 Å), the cross sections for the photoionization of nitrogen used in the air radiation calculations of the present work ("Burgess-Seaton general formula; semiempirical phase shifts") fall off too rapidly with decreasing photon wavelength. In view of the fact that Bates and Seaton used hydrogen wave functions in obtaining the energy dependence of their cross sections, we carried out a further calculation, according to the Burgess-Seaton formula, identical to the first except that the extrapolated quantum defects for the continuum were set equal to zero. The results are shown in figure 8. A slight improvement in the shape of the curve is noticeable, but the threshold cross section is now somewhat lower. Within the context of the Burgess-Seaton method and general formula it would seem, therefore, that better agreement of calculated cross sections with experiment is unlikely to be obtained with improved knowledge of the phase shifts alone (we remind the reader of the averaging process which was done to obtain eqs. (19a,b)).

It may be that the Coulomb approximation-quantum defect method is incapable of predicting fairly precise photoionization cross sections for nitrogen and oxygen atoms. Before this can be concluded, however, it should be noted that the Burgess-Seaton general formula (the values of the various parameters in reference 3 being considered as part of the formula) would not necessarily be a precise rendering of the Coulomb approximation even if the phase shifts were known "exactly." In developing their formula, Burgess and Seaton used, as a first approximation for the regular and irregular continuum Coulomb wave functions, the first two terms in the respective series expansions in powers of the energy (about zero energy) of these analytic functions. At this point in the calculation their results could only give accurate matrix elements at or very near threshold, so they undertook to find a functional form involving parameters, and the appropriate values of those parameters, in order to generate a formula which gave bound-free matrix elements in agreement with the complete Coulomb approximation for energies well above threshold. In particular, they introduced the parameters $\gamma_{l,l'}(n^*)$ as shown in equation (13).

To assess the validity of the Burgess-Seaton formula, Anderson and Griem (ref. 30) compared the cross sections predicted by this formula for photoionization of hydrogen with the exact results. They found that the cross sections derived from the Burgess-Seaton formula (1) were accurate at threshold for photoionization of H(1s,2s,2p,3s,3p,3d); (2) agreed to within about 5 percent

up to three times the respective threshold energy for H(2s,3s); (3) were in fair agreement for H(1s,2p,3p) up to three times the corresponding threshold energy, an agreement which was considerably improved by changing the values of some of the parameters in the Burgess-Seaton formula; (4) were in increasing disagreement for H(3d) photoionization cross sections for energies increasing beyond threshold, a disagreement which no consistent set of revised parameters could rectify. In particular, they found that for photoionization of H(2p,3p), small (usually downward) changes of $\gamma_{12}(n^*)$, $1.8 \leq n^* \leq 3.0$, with a concomitant change in α_{12}, brought the cross sections calculated with the Burgess-Seaton formula into better agreement with the exact results in the energy range considered.

As we have mentioned, transitions to final d wave states tend to be more probable than transitions to final s wave states for the photoionization processes considered in the present work. A downward revision of the parameter $\gamma_{12}(n^*)$, $n^* \cong 1.0$, from the values given in reference 1, would have the effect of making the cross sections for all these processes fall off less rapidly with decreasing photon wavelength, while leaving the threshold values unchanged. Given that the general shape of Ehler and Weissler's empirical cross-section curve is correct, it would certainly be of interest to ascertain whether a more precise treatment of the Coulomb approximation would in fact have the effect of decreasing $\gamma_{12}(n^*)$ for this transition in nitrogen. An investigation of the possible changes of this and other parameters from the values given in reference 1, or of more general alterations in the Burgess-Seaton formula, either of which may result from a more precise use of the Coulomb approximation, is beyond the scope of the present work, however.

We conclude these comments on nitrogen, and on the energy dependence of the photoionization cross sections, by remarking that for lower temperatures ($T \lesssim 15{,}000^\circ$ K) most of the light arising from processes considered here comes from recombination of low energy electrons with N^+ and O^+ ions, so that the integrated radiation rate of air is most sensitive to the corresponding photoionization cross sections near threshold. For temperatures above $15{,}000^\circ$ K the (possibly) excessive rate of decrease (with decreasing wavelength) of the photoionization cross sections used in the present calculation will give rise to an increasing percentage underestimate of the radiation rate of air as $B_\lambda(T)$ flattens out in the wavelength region $400 \text{ Å} \leq \lambda \leq 1{,}130 \text{ Å}$.

We now turn to the question of the threshold cross section for the process photon + $1s^2 2s^2 2p^4(^3P) \rightarrow 1s^2 2s^2 2p^3(^4S^o)$ + free electron, in atomic oxygen. Bates and Seaton (ref. 27), using Hartree-Fock wave functions and the dipole length formula, obtained a value 2.3×10^{-18} cm^2, whereas we calculated a value 5.1×10^{-18} cm^2 using the Burgess-Seaton formula with semiempirical energies and phase shifts. The disagreement is striking, all the more so in view of the good agreement of the nitrogen ground state threshold cross sections calculated in reference 27 and the present work (10.2×10^{-18} cm^2 and 11.0×10^{-18} cm^2, respectively).

As a first step in resolving this disagreement we calculated the cross sections for this oxygen process using the Burgess-Seaton formula, the Hartree-Fock energy (ref. 31) for the 2p wave function, and Hartree-Fock

phase shifts (quoted in ref. 12) for the continuum functions. The value so calculated was 1.8×10^{-18} cm^2, a result in fair agreement with the Bates-Seaton value of 2.3×10^{-18} cm^2.

The reasons why this change in input into the Burgess-Seaton formula results in so great a difference in cross sections are: (1) the value of the cosine in equation (12) is sensitive to changes in the argument for this process for $l' = 2$; (2) the Hartree-Fock value for n^* (= effective principal quantum number for a 2p orbital for this transition) is 0.890, while the experimental value is 1.000. The Hartree-Fock and experimental values of n^* for 2p electrons in the ground state of atomic nitrogen are 0.942 (ref. 28) and 0.967, respectively, which helps to explain the relatively close agreement of the two estimates of the nitrogen threshold cross sections.

It is interesting to consider the underlying reason that the agreement between the Hartree-Fock and experimental n^* values is poorer for oxygen $2p^4(^3P)$ than for nitrogen $2p^3(^4S^o)$. We note that the n^* values are determined by the asymptotic forms of the wave functions (see appendix A). If one of the 2p electrons in $2p^3(^4S^o)$ is at a great distance from the nucleus, the remaining core must be $2p^2(^3P)$ and not $2p^2(^1D$ or $^1S)$ on account of (at least) the differences in spins. On the other hand, if the radius of one of the electrons in $2p^4(^3P)$ becomes large, the remaining three electrons may be found in states of $2p^3(^4S^o,^2D^o,^2P^o)$ with probabilities of roughly 1/3, 5/12, 1/4, respectively, these numbers being the squares of the corresponding coefficients of fractional parentage (refs. 32 and 33). The Hartree-Fock approximation for $2p^4(^3P)$ treats the core terms $2p^3(^4S^o,^2D^o,^2P^o)$ as if they had the same energy; if, in fact, second-order changes in energy (due to small changes in the Hartree-Fock 2p wave function between the configurations $2p^4$ and $2p^3$) are neglected, the Hartree-Fock energy parameter ($|\epsilon| = 1/n^{*2}$) will estimate the weighted average difference in energies between $2p^4(^3P)$ and $2p^3(^4S^o,^2D^o,$ $^2P^o)$, the weighting factors being the squares of the respective fractional parentage coefficients.[7] Using the experimental energy differences (ref. 4) we have (in Rydberg units)

$$\frac{1}{3}(1.0002) + \frac{5}{12}(1.2446) + \frac{1}{4}(1.3690) = 1.194$$

which is in fair agreement with the Hartree-Fock value of 1.262 (ref. 31).

On the basis of this information, it seems reasonable to conclude that the cross sections, calculated with Hartree-Fock wave functions, for photoionization of p^q by ejection of an electron leaving a p^{q-1} core, are probably unreliable when the initial term of p^q has more than one parent term among the terms of p^{q-1}, if the differences in energies among the parent terms of p^{q-1} are not small compared to the threshold energy for photoionization.

---

[7]This assertion may be verified for this and other terms of p^3, p^4 configurations with the help of the theory developed in reference 32, vol. II.

With respect to the above discussion of photoionization cross sections and in the light of what has gone before, the following tentative over-all conclusions may be drawn: (1) Subject to revision depending on the outcomes of experiments or of more accurate calculations, the Burgess-Seaton general formula is probably capable of giving fair to good threshold cross sections for the nitrogen and oxygen processes considered here if the correct phase shifts, etc., are used. In this connection, a closer investigation of series energy levels for nitrogen and oxygen, and of extrapolation of the quantum defects to the continuum, particularly for series where the ionic core has fine structure, is needed (some of the theoretical groundwork has been laid in ref. 34; see also ref. 9); also, the values of some of the parameters for the general formula are rapidly varying functions of n^*, and are tabulated (in ref. 3) on a mesh of points too coarse for certain extrapolation or interpolation. (2) In the one case where experimental photoionization cross sections are approximately known, the cross sections derived from the Burgess-Seaton formula seem to fall off too rapidly with decreasing photon wavelength. The simplest explanation of this discrepancy leads to the conclusion that the same excessively rapid fall-off of the calculated cross sections may be true for all the processes treated here. A careful investigation of the Coulomb approximation for bound-free matrix elements must be undertaken to ascertain whether this (presumed) error lies in the Coulomb approximation itself or in the values specified by Burgess and Seaton for the parameters in their general formula.[8]

Discussion of Air Radiation Calculations

A few remarks are in order on the parts of the air radiation calculations of Nardone, Breene, Zeldin, and Riethof (ref. 1), and of Sewell (ref. 2), which are comparable with the results of the present work.

---

[8]Late in the preparation of this paper, it has come to our attention that Peterson (ref. 35) has calculated photoionization cross sections for (among others) the processes treated in the present work. Peterson, who also used the Burgess-Seaton general formula, calculated cross sections which differ (in some cases considerably) from those obtained here. The discrepancy may lie in part in the fact that Peterson has throughout (incorrectly) interpreted the extrapolated quantum defects $\mu'(\epsilon')$ of the final continuum states to be the extrapolated quantum defects of the same series of atomic energy levels as that which contains the initial, bound state as a member. However, Peterson essentially cancels out this error for photoionization from the configuration $2p^q$ $(q > 1)$ by putting all the $\mu'(\epsilon') = 0$ for $\epsilon' \geq 0$. Substituting $\mu'(\epsilon') = 0$ for all the continuum states in our own calculation tends to lower our cross sections and improve agreement with Peterson's; the differences, however, are still considerable. We believe that Peterson's cross-section values are too low. For example, he obtains a value 2.03×10^{-18} cm^2 for the threshold cross section for neutral nitrogen (threshold wavelength 852 Å), and 0.011×10^{-18} cm^2 for the threshold cross section for neutral oxygen (threshold wavelength 911 Å). However, we have been unable to deduce the means by which these values were obtained.

Sewell used the version of the Kramers approximation given in table I of reference 23, but did not account for screening; that is, in the notation of appendix C, Sewell put $Z_{eff} = \zeta$. Nardone, et al., apparently used a kind of hydrogen approximation for their matrix elements, taking the over-all wave functions to be single determinant wave functions[9] which are not necessarily eigenfunctions of L, S, or J. Some threshold cross sections for photoionization processes inferred from the graphs of Nardone, et al. (ref. 1, figs. 71 and 74; curves for $T = 10{,}000^{\circ}$ K) are given in table I.

Apparently neither the results of reference 1 nor those of reference 2 included recombination of electrons with N^+ or O^+ ions which were not in the lowest energy terms of their respective ground configurations. Processes of this sort, however, were found in the present investigation to add relatively little to the total rate of light emission, particularly at lower temperatures, of course. Sewell apparently does not take into account light arising from

$$2p^2(^3P) + \text{free electron} \rightarrow 2p^3(^4S^{\circ}) + \text{photon}$$

in nitrogen (threshold at 852 Å), and

$$2p^3(^4S^{\circ}) + \text{free electron} \rightarrow 2p^4(^3P) + \text{photon}$$

in oxygen (threshold at 911 Å). On the other hand both Sewell and Nardone, et al., show contributions resulting from the processes

$$2p^3(^4S^{\circ}) + \text{free electron} \rightarrow 2p^4(^1D) + \text{photon}$$

in oxygen (threshold at 1064 Å) and

$$2p^3(^4S^{\circ}) + \text{free electron} \rightarrow 2p^4(^1S) + \text{photon}$$

also in oxygen (threshold at 1315 Å). Both transitions are forbidden if small magnetic effects in oxygen are neglected.

Figure 9 compares the integrated emission coefficient for air as obtained in each of the three calculations, for $\rho/\rho_o = 10^{-3}$ (our results are not easily comparable with those of Nardone, et al., at higher densities). For this density, the value of $J(\lambda_1,\lambda_2) = \int_{\lambda_1}^{\lambda_2} J_\lambda d\lambda$ for the N^+ electron and O^+ electron recombination light (principally in the vacuum ultraviolet) from heated air is in reference 1 typically twice that of the present work, and in reference 2 typically one-third that of the present work.[10]

---

[9]Private communication from R. G. Breene

[10]The limits on the integration over J_λ are 400 Å and 1,130 Å in the present work, 500 Å to 2,000 Å in reference 1, and about 850 Å to 17,000 Å in reference 2. The $J(\lambda_1,\lambda_2)$ of reference 2 includes recombination into other excited states of N and O. Nardone, et al. (ref. 1) did not define ρ_o nor give the source of their data on the composition of air. We assume their ρ_o to be the same as ours, 1.225×10^{-3} g cm^{-3}.

CONCLUDING REMARKS

The photoionization cross sections for certain levels of nitrogen and oxygen atoms have been calculated with the Burgess-Seaton general formula (ref. 3). These results were, in turn, used to estimate the rate of emission of light by air due to the reverse, recombination processes, at temperatures from 8,000° K to 24,000° K, densities from 10^{-6} to 10^{2} times normal, and integrated over wavelengths from 400 Å to 1,130 Å. Also, a table of data was obtained which facilitates estimation of the emitted flux of radiation at the surface of uniform thick bodies of air.

The photoionization cross sections were compared with the results of other calculations and the results of the only known relevant experiment (ref. 26). The values of the nitrogen ground state photoionization cross section obtained in the present calculation fell within, but near the limits of, the range of experimental values (including estimated systematic errors) as determined by Ehler and Weissler. The theory of Bates and Seaton (ref. 27) gave results in better agreement with this experiment as regards the shape of their cross section versus wavelength curve. An explanation for the discrepancy was proposed and discussed, namely that the Burgess-Seaton formula may not be an accurate representation of the Coulomb approximation for bound-free transitions not close in energy to threshold.

With respect to the estimates of air radiation, these results were compared with those of Nardone, et al. (ref. 1), and of Sewell (ref. 2), who used a hydrogen type approximation and Kramers formula (ref. 23), respectively. For $\rho/\rho_o = 10^{-3}$, the predicted rate of (mostly vacuum ultraviolet) light emission by air due to N^+, O^+ electron recombination (the processes included differed somewhat among the three works) was calculated by Nardone, et al., to be about twice, and by Sewell to be about one-third that calculated here for $8{,}000° \text{ K} \leq T \leq 24{,}000° \text{ K}$.

Ames Research Center
National Aeronautics and Space Administration
Moffett Field, Calif., Feb. 2, 1965

APPENDIX A

DETERMINATION OF SEMIEMPIRICAL ENERGY PARAMETERS AND REMARKS ON THE COULOMB APPROXIMATION

It is possible to sharpen the justification given by Bates and Damgaard (ref. 8) for their prescription for calculating the bound state energy parameters E from observed atomic energy levels. They proposed that, for an electron in a given $n\ell$ shell in the atom, $|E|$ be taken as the energy required to remove that electron from the atom. In fact, it is reasonable to use a value of E which depends both on the initial state of the atom, and on the energy state of the residual core of the atom, the core being taken as approximately unchanged in a radiative transition. To see how this comes about, it is convenient to begin with the Schrödinger equation for the energy eigenstate of the atom of interest (nonelectrostatic interactions are neglected):

$$\left[\sum_{i=1}^{N}\left(-\nabla_i^2 - \frac{2Z}{r_i}\right) + \sum_{i=1}^{N}\sum_{j=i+1}^{N}\frac{2}{r_{ij}}\right]\Psi = E_T\Psi \tag{A1}$$

where N is the number of electrons, Z is the charge of the nucleus, r_i and r_{ij} are the distances of the ith electron from the nucleus and jth electron, respectively, and the wave function Ψ, a function of $3N$ coordinates (spin coordinates are suppressed), satisfies the boundary conditions for a bound state of the atom with total energy E_T (in Rydberg units).

As the distance from the nucleus of one of the electrons, say the first, becomes large, the difference between r_1 and r_{1j}, $j = 2, \ldots, n$, becomes relatively small, so that for r_1 large,

$$\left[-\nabla_1^2 - \frac{2(Z - N + 1)}{r_1} + \sum_{i=2}^{N}\left(-\nabla_i^2 - \frac{2Z}{r_i}\right) + \sum_{i=2}^{N}\sum_{j=i+1}^{N}\frac{2}{r_{ij}}\right]\Psi = E_T\Psi \tag{A2}$$

to a first approximation. To the same accuracy, then, the wave function must tend in this limit to a sum of functions $\Psi_\alpha(\underline{r_1}, \ldots, \underline{r_N})$ each of which is a product function of a function $\varphi_\alpha(\underline{r_1})$ and a function $\Phi_\alpha(\underline{r_2}, \ldots, \underline{r_N})$ that is,

$$\Psi(\underline{r_1}, \ldots, \underline{r_N}) \xrightarrow[r_1 \to \infty]{} \sum_\alpha \varphi_\alpha(\underline{r_1})\,\Phi_\alpha(\underline{r_2}, \ldots, \underline{r_N}) \tag{A3}$$

Furthermore, Φ_α and φ_α must satisfy, respectively,

$$\left[\sum_{i=2}^{N}\left(-\nabla_i^2 - \frac{2Z}{r_i}\right) + \sum_{i=2}^{N}\sum_{j=i+1}^{N}\frac{2}{r_{ij}}\right]\Phi_\alpha = E_\alpha\Phi_\alpha \tag{A4}$$

and

$$\left(-\nabla_1^2 - \frac{2\zeta}{r_1}\right)\varphi_\alpha(\underline{r_1}) = (E_T - E_\alpha)\varphi_\alpha(\underline{r_1}) \tag{A5}$$

where $\zeta = Z - N + 1$. It is clear that the E_α and Φ_α must be eigenvalues and eigenfunctions of the $N - 1$ electron core.[1] The value $E_T - E_\alpha$ becomes, on further separation of variables in equation (5a), the E parameter in the resulting radial wave equation, where the radial wave function has its asymptotic form given by equation (7); that is,

$$r_1\varphi_\alpha(\underline{r_1}) \sim \text{const} \times r_1^{n^*}e^{-r_1/n^*} \times (\text{eigenfunction of } \underline{L_1}^2 \text{ with eigenvalue } l(l+1)) \tag{A6}$$

where

$$n^* = \frac{\zeta}{\sqrt{E_\alpha - E_T}}$$

The energy states of the $N - 1$ electron core corresponding to the eigenfunctions Φ_α are the "parents" of the state (with wave function Ψ) of the N electron atom, and while x-ray terms, the continuum and other highly excited states of the core, may appear in the sum in equation (A3), the corresponding φ_α will be rapidly decreasing exponentials with, in some sense, "small" amplitudes.

A similar asymptotic form exists for the final, continuum states of the photoionization process, with the difference that here at least one of the $E_T - E_\alpha$ is positive, and correspondingly r_1 times the radial part of φ_α behaves as in equation (6). If we now approximate the matrix element of the position operator by neglecting the contribution for small r_1, the expansion of equation (A3) may be used for the wave functions; nonzero contributions to the matrix element will come from overlap of the parts of the initial and final wave functions for which the ionic core is in the same state. (If appropriate changes are made, identical contributions will be obtained for large $r_2, r_3, \ldots, r_N$.) Only the core states which appear in a single configuration approximation, such as the Hartree-Fock model, will be considered here, however.

None of this gives any information on the (implicity given) normalization constants of the terms in the asymptotic form for Ψ (eq. (A3)). Approximate

---

[1]A result used (also without proof) by Bely, Moores, and Seaton (ref. 34).

values for some of these constants may be calculated from the quantum defect method (ref. 7), or from solutions of the Hartree-Fock equations for the atom.

APPENDIX B

ROUGH PROOF OF RELATION (41) AND OF THE STATEMENT FOLLOWING

The essential result to be obtained can be expressed simply. Given real functions $f(x)$ and $w(x)$ defined and bounded in absolute value for $a \leq x \leq b$, $a < b$; assume f integrable, w continuous (and therefore integrable),

$$w(x) > 0 \quad \text{for} \quad a \leq x \leq b \tag{B1}$$

and

$$\int_a^b f(x)w(x)dx = 0 \tag{B2}$$

let α be a real number, θ be a positive real number, and let

$$\delta = \theta \int_a^b [f(x)]^2 w(x)dx \tag{B3}$$

$$g(\alpha) = \int_a^b (e^{\alpha f(x)} - 1)w(x)dx \tag{B4}$$

Then it follows that

$$g(\alpha) \geq 0 \tag{B5}$$

where the equality holds identically in (B5) if and only if $\delta = 0$, and, if $\delta \neq 0$, the equality holds if and only if $\alpha = 0$.

Proof: The restrictions put on f and w imply first, that the integrals in (B2), (B3), and (B4) exist; second, that

$$\int_a^b w(x)dx > 0 \tag{B6}$$

and third, that the derivatives of $g(\alpha)$ with respect to α exist and that differentiation and integration can be interchanged on the right-hand side of (B4). In particular,

$$g'(\alpha) = \int_a^b f(x)e^{\alpha f(x)}w(x)dx \tag{B7}$$

and

$$g''(\alpha) = \int_a^b [f(x)]^2 e^{\alpha f(x)} w(x)dx \tag{B8}$$

Evidently $g(0) = g'(0) = 0$ and $g''(\alpha) \geq 0$ for any α. In fact if, for any particular α, $g''(\alpha) = 0$, then $f(x)$ must be zero almost everywhere for $a \leq x \leq b$.

According to Taylor's theorem, if $n \geq 1$ is an integer and the nth derivative $g^{(n)}(\alpha)$ exists and is finite everywhere in the open interval (c,d), and $g^{(n-1)}(\alpha)$ is continuous in the closed interval $[c,d]$, then for any $\alpha\epsilon(c,d)$ there is an interior point α_o, $c < \alpha_o < \alpha$, such that

$$g(\alpha) = g(c) + \sum_{k=1}^{n-1} \frac{g^{(k)}(c)}{k!} (\alpha - c)^k + \frac{g^{(n)}(\alpha_o)}{n!} (\alpha - c)^n$$

The conditions of Taylor's theorem are satisfied for $g(\alpha)$ as defined in (B4) if $c = 0$, $d > 0$, and $n = 2$. Thus for $0 < \alpha < d$, there is an α_o, $0 < \alpha_o < \alpha$, such that

$$g(\alpha) = (1/2)g''(\alpha_o)\alpha^2 \tag{B9}$$

Since $g''(\alpha_o)$ is non-negative for all α_o, $g(\alpha) \geq 0$ for $0 < \alpha < d$. But d is positive and otherwise arbitrary so that $g(\alpha) \geq 0$ if $\alpha > 0$. An argument similar to the above for $h(\alpha) = g(-\alpha)$ shows $g(\alpha) \geq 0$ for $\alpha < 0$. Since $g(0) = 0$, $g(\alpha) \geq 0$ for all α.

If $\delta = 0$ then $f(x) = 0$ almost everywhere and $g''(\alpha) = 0$ for all α. By (B9) and its extension for $\alpha < 0$, and since $g(0) = 0$, $g(\alpha) = 0$ for all α. Conversely, if g is identically zero, then $g''(0)$ must be zero, and hence $\delta = 0$.

Whatever the value of δ, $\alpha = 0$ implies $g(\alpha) = 0$. If $g(\alpha) = 0$ for some $\alpha \neq 0$, say α_1, and $\delta \neq 0$, then by (B9), or its extension to negative α, there is an α_o such that $0 < \alpha_o < \alpha_1$ if $\alpha_1 > 0$, or $\alpha_1 < \alpha_o < 0$ if $\alpha_1 < 0$, and

$$g(\alpha_1) = 1/2\ g''(\alpha_o)\alpha_1^2 \tag{B10}$$

But $\alpha_1 \neq 0$ and $g''(\alpha_o) \neq 0$ since $\delta \neq 0$, so the assumption that $g(\alpha_1) = 0$ for $\alpha_1 \neq 0$ leads to a contradiction. Hence, if $\delta \neq 0$, $g(\alpha)$ can be zero only if $\alpha = 0$, and the proof of the theorem is complete.

To apply the results of the theorem to the statement in the text, multiply relation (41) by $\exp[\bar{k}(\lambda_1,\lambda_2)L]$ and let

$$\alpha = L$$

$$x = \lambda,\ a = \lambda_1,\ b = \lambda_2$$

$$f(x) = \bar{k}(\lambda_1,\lambda_2) - k_\lambda$$

$$w(x) = B_\lambda$$

$$\theta = \left[\bar{k}(\lambda_1,\lambda_2)^2 \int_{\lambda_1}^{\lambda_2} B_\lambda d_\lambda\right]^{-1}$$

$$\delta = \Delta$$

The assertions in this appendix have been based on theorems stated in (1) F. Riesz and B. Sz-Nagy, "Functional Analysis," Ungar, New York (1955); (2) E. T. Whittaker and G. N. Watson, "A Course of Modern Analysis," McMillan, New York (1947); (3) T. M. Apostol, "Lectures in Advanced Calculus," California Institute of Technology, Pasadena, California (1954).

APPENDIX C

THE KRAMERS FORMULA

Kramers semiclassical approximation (ref. 36) for the cross section for photoionization of a hydrogen-like atom is

$$\sigma = \frac{64\pi^4}{3\sqrt{3}} \frac{e^{10} m Z^4}{h^6 c \nu^3 n^5} \tag{C1}$$

where Z is the atomic number of the nucleus, ν is the frequency (exceeding threshold) of the photon, and n is the principal quantum number of the electron in its initial bound state.

To the end of obtaining a simple formula for estimating photoionization cross sections for many electron atoms, we first introduce an effective Z and, second, apply a multiplicative correction to the right side of (C1), in order to account for the differences in ionization energies and in structural properties, respectively, between one-electron and many-electron atoms.

We make the following (by no means unique) choice of an effective Z, which is suggested in reference 23: If $I_{n\ell}$ is the threshold energy (in Rydbergs) for a photoionization process of the atom of interest in which an $n\ell$ electron is ejected and initial atom and final ion core are in definite or approximate energy levels, we choose

$$Z = Z_{eff} = n\sqrt{I_{n\ell}} \tag{C2}$$

Thus Z_{eff} depends on the photoionization process considered, except for hydrogen-like atoms.

Making use of this definition of $Z = Z_{eff}$, (C1) can be brought into the form of equation (11) in the text:

$$\sigma = \frac{4\pi}{3} \alpha a_o^2 \frac{I_{n\ell} + k^2}{I_{n\ell}^2} \left[\frac{16}{n\sqrt{3}} \left(\frac{I_{n\ell}}{I_{n\ell} + k^2} \right)^4 \right] \tag{C3}$$

where $I_{n\ell} + k^2$ is the energy (in Rydbergs) of the incoming photon. The term in brackets in (C3) corresponds to the sum in (11); n is still the integral principal quantum number of the initial state of the jumping electron. We define the unmodified Kramers formula to mean (C3).

When the ejected electron is equivalent with other electrons in the initial state (and all $n\ell$ shells containing electrons are closed other than the $n\ell$ shell containing the ejected electron), we note in equation (16) of

reference 3 that the only change in the constants $C_{l'}$ (see eq. (1) in the text) from the inequivalent electron case is that they are multiplied by the l'-independent quantity

$$q\left|\left(l^{q}SL\{\,|\,l^{q-1}(S''L'')\,lSL\right)\right|^{2}$$

Here q is the number of equivalent electrons in the initial nl shell of the jumping electron and $\left(l^{q}SL\{\,|\,l^{q-1}(S''L'')\,lSL\right)$ is a coefficient of fractional parentage (refs. 3, 32, and 33); l is the initial angular momentum quantum number of the jumping electron, and SL, $S''L''$ are total spin and total orbital angular momentum of the initial atom and final ion core, respectively.

This fact suggests the writing of the following "modified" Kramers formula (adapted from Armstrong, Holland, and Meyerott, ref. 37):

$$\sigma = \frac{4\pi}{3}\alpha a_{o}^{2}\left(\frac{I_{nl}+k^{2}}{I_{nl}^{2}}\right)\left[q\left|\left(l^{q}SL\{\,|\,l^{q-1}(S''L'')\,lSL\right)\right|^{2}\frac{16}{n\sqrt{3}}\left(\frac{I_{nl}}{I_{nl}+k^{2}}\right)^{4}\right] \qquad (C4)$$

If the ejected electron is not equivalent with other electrons, $q = 1$, the fractional parentage coefficient is 1, and the cross-section formula reduces to (C3).

These modifications can at best account for only the grossest properties of many-electron atoms. Nevertheless, the few examples given in table I and figure 8 show that at least for threshold cross sections, the values obtained by the modified Kramers formula are in fair to good agreement with cross sections calculated with the more elaborate Burgess-Seaton general formula. That this is the case is not necessarily surprising since it might be expected that the quantities $g(n^{*}l;\epsilon'l')$ (defined in eq. (10) in the text), in view of their lack of explicit dependence on atomic number Z or on ζ (see symbols), would be insensitive to changes in Z or ζ, particularly for 2p continuum d wave transitions. Most of the differences in cross sections among the transitions treated in this paper are due to differences in threshold energies, fractional parentage coefficients, and numbers of electrons in the 2p shell.

REFERENCES

1. Nardone, M. C.; Breene, R. G.; Zeldin, S. S.; and Riethof, T. R.: Radiance of Species in High Temperature Air. General Electric Co., Space Sciences Lab. Rep. R 63 SD3, June 1963.

2. Sewell, K. G.: The Radiative Properties of Air in Thermodynamic Equilibrium. Ling-Temco-Vought Research Center Rep. 0-71000/2R-26, July 1962.

3. Burgess, A.; and Seaton, M. J.: A General Formula for Calculation of Atomic Photo-Ionization Cross Sections. Monthly Notices Roy. Astron. Soc., vol. 120, no. 2, 1960, pp. 121-151.

4. Moore, Charlotte E.: Atomic Energy Levels, Volumes I, II, III, NBS Circular 467.

5. Ditchburn, R. W.; and Öpik, U.: Photoionization Processes. Atomic and Molecular Processes, ed. D. R. Bates, Academic Press, N.Y., 1962, pp. 79-99.

6. Zhigulev, V. N.; Romishevskii, Ye. A.; and Vertushkin, V. K.: Role of Radiation in Modern Gasdynamics. AIAA Jour., vol. 1, no. 6, June 1963, pp. 1473-1485.

7. Seaton, M. J.: The Quantum Defect Method. Monthly Notices Roy. Astron. Soc., vol. 118, no. 5, 1958, pp. 504-518.

8. Bates, D. R.; and Damgaard, Agnete: The Calculation of the Absolute Strengths of Spectral Lines. Phil. Trans. Roy. Soc., vol. 242, no. 842, July 1949, pp. 101-122.

9. Edlén, Bengt: Atomic Spectra. Handbuch der Physik, vol. XXVII, S. Flügge, ed., Springer, Berlin, 1964, pp. 80-220.

10. Hylleraas, Egil A.: Evaluation of Transition Probabilities for Non-Coulombian Central Fields, Arkiv for Mathematik og Naturvidenskab, vol. 48, no. 4, 1946, pp. 57-88.

11. Seaton, Michael John: Le Calcul approximatif des sections efficaces de photo-ionisation atomique. I. L'emploi des fonctions d'onde hydrogénoïdes pour les états continus. Académie des Sciences, Paris, Comptes Rendus, vol. 240, no. 11, March 1955, pp. 1193-1195.

12. Seaton, Michael John: Le Calcul approximatif des sections efficaces de photoionisation atomique II. Une relation entre le défaut quantique et la phase de la fonction d'onde à la limite spectrale. Académie des Sciences, Paris, Comptes Rendus, vol. 240, no. 12, March 1955, pp. 1317-1318.

13. Ham, Frank S.: The Quantum Defect Method. Vol. I of Solid State Physics, Frederick Seitz and David Turnbull, eds., Academic Press, N.Y., 1955, pp. 127-192.

14. Moiseiwitsch, B. L.: On the Relation between Phase Shift and Quantum Defect. Proceedings of the Physical Society, vol. 79, pt. 6, no. 512, June 1962, pp. 1166-1169.

15. Norman, G. E.: A Basis for the Quantum Defect Method. Optics and Spectroscopy, vol. 12, no. 3, 1962, pp. 183-185.

16. Burgess, A.; and Seaton, M. J.: Cross Sections for Photoionization from Valence-Electron States. Rev. Mod. Phys., vol. 30, no. 3, July 1958, pp. 992-993.

17. Norman, G. E.: Photoionization Cross Sections of the Lower Excited States and Oscillator Strengths of Certain Lines of Carbon and Nitrogen Atoms. Optics and Spectroscopy, vol. 14, no. 5, May 1963, pp. 315-317.

18. Kvifte, G.: An Extension of the Normal Series of the OI Spectrum. Archiv for Mathematik og Naturvidenskab, vol. 52, no. 4, 1952, pp. 65-68.

19. Eriksson, Karl Börje S.; and Isberg, H. Bengt S.: O I Quintet and Triplet Terms Below the Ionization Limit. Arkiv för Fysik, vol. 24, no. 41, 1963, pp. 549-558.

20. Eriksson, Karl Börje S.: Revised Energy Levels for the Neutral Nitrogen Atom. Arkiv för Fysik, vol. 13, no. 34, 1958, pp. 429-439.

21. Eriksson, Karl Börje S.; and Johansson, Ingmar: The Spectrum of the Neutral Nitrogen Atom in the Lead-Sulfide Region. Arkiv för Fysik, vol. 19, no. 16, 1961, pp. 235-248.

22. Sewell, et al.: Thermodynamic Properties of High Temperature Air. Chance-Vought Research Center Rep. Re-Ir-14, June 1961.

23. Finkelnburg, W.; and Peters, Th.: Kontinuierliche Spektren. Handbuch der Physik, vol. XXVIII, S. Flügge, ed., Springer, Berlin, 1957, pp. 79-204.

24. Unsöld, Albrecht: Physik der Sternatmosphären. Springer, Berlin, 1955.

25. Chandrasekhar, S.: Radiative Transfer, Dover Pub., N.Y., 1960.

26. Ehler, A. W.; and Weissler, G. L.: Ultraviolet Absorption of Atomic Nitrogen in its Ionization Continuum. J. Opt. Soc. Am., vol. 45, no. 12, Dec. 1955, pp. 1035-1043.

27. Bates, D. R.; and Seaton, M. J.: The Quantal Theory of Continuous Absorption of Radiation by Various Atoms in Their Ground States. II. Further Calculations on Oxygen, Nitrogen, and Carbon. Monthly Notices of the Roy. Astron. Soc., vol. 109, no. 6, 1949, pp. 698-704.

28. Hartree, D. R.; and Hartree, W.: Self-Consistent Field, With Exchange, for Nitrogen and Sodium. Proc. Roy. Soc., Ser. A193, no. 1034, July 1948, pp. 299-304.

29. Bates, D. R.: An Approximate Formula for the Continuous Radiative Absorption Cross-Sections of the Lighter Neutral Atoms and Positive and Negative Ions. Monthly Notices Roy. Astron. Soc., vol. 106, no. 5, 1946, pp. 423-431.

30. Anderson, A. D.; and Griem, H. R.: Continuum Emission Coefficients From the Quantum Defect Method. Comptes Rendus de la VI. Conférence Internationale sur les Phénomènes D'Ionization Dans Les Gaz, vol. III, P. Hubert and E. Crémieu-Alcan, eds., Paris, July 1963, pp. 293-298.

31. Hartree, D. R.; Hartree, W.; and Swirles, Bertha: Self-Consistent Field, Including Exchange and Superposition of Configurations, With Some Results for Oxygen. Phil. Trans. Roy. Soc. of London, Ser. A238, no. 790, July 1939, pp. 229-247.

32. Slater, John C.: Quantum Theory of Atomic Structure. Vols. I and II, McGraw-Hill Book Co., 1960.

33. Rohrlich, F.: Theoretical Multiplet Strengths. Astrophys. J., vol. 129, no. 2, March 1959, pp. 441-448.

34. Bely, O.; Moores, D.; and Seaton, M. J.: Many-Channel Quantum Defect Theory. Atomic Collision Processes, M. R. C. McDowell, ed., North Holland, Amsterdam, 1964, pp. 304-311.

35. Peterson, Earl: The Calculation of Photo-Ionization Cross Sections by the Quantum Defects Method. GM Defense Res. Lab. Rep. TR 64-02B, April 1964.

36. Kramers, H. A.: On the Theory of X-Ray Absorption and of the Continuous X-Ray Spectrum. Phil. Mag., vol. 46, 1923, pp. 836-871.

37. Armstrong, Baxter, H.; Holland, Dan H.; and Meyerott, Roland E.: Absorption Coefficients of Air From 22,000° to 220,000°. Lockheed Aircraft Corp. LMSD S135, AFSWC TR 58-36, Aug. 1958.

38. Yamanouchi, Takahiko; and Kotani, Masao: Photo-Ionization and Recombination of Oxygen Atom. Proc. Phys. Math. Soc. Japan, vol. 22, 1940, pp. 60-76.

TABLE I.- COMPARISON OF CALCULATED THRESHOLD PHOTOIONIZATION CROSS SECTIONS

Atom	Process	Threshold wavelength	Author	Threshold cross section (in 10^{-18} cm^2)	Comments
NI	Photon + $2p^3(^4S^o) \rightarrow 2p^2(^3P) + e^-$	852 Å	This paper	11.0	Burgess-Seaton general formula[a]
				11.1	Modified Kramers approximation
			Bates and Seaton (ref. 27)	10.2	Dipole length } Hartree-Fock
				7.7	Dipole velocity } wave functions
			Nardone, et al. (ref. 1)	20 ± 3	Inferred from emissivity data in reference 1, figure 74
NI	Photon + $2p^3(^2D^o) \rightarrow 2p^2(^3P) + e^-$	1020 Å	This paper	8.4	Burgess-Seaton general formula[a]
				6.6	Modified Kramers approximation
			Nardone, et al. (ref. 1)	26 ± 3	Inferred from emissivity data in reference 1, figure 74
NI	Photon + $2p^3(^2P^o) \rightarrow 2p^2(^3P) + e^-$	1130 Å	This paper	11.1	Burgess-Seaton general formula[a]
				7.35	Modified Kramers approximation
			Nardone, et al. (ref. 1)	38 ± 4	Inferred from emissivity data in reference 1, figure 74
OI	Photon + $2p^4(^3P) \rightarrow 2p^3(^4S^o) + e^-$	911 Å	This paper	5.1	Burgess-Seaton general formula[a]
				5.3	Modified Kramers approximation
			Bates and Seaton (ref. 27)	2.3	Dipole length } Hartree-Fock
				2.8	Dipole velocity } wave functions
			Yamanouchi and Kotani (ref. 38)	4.5	Hartree self-consistent field wave functions, dipole length formula
			Nardone, et al. (ref. 1)	34 ± 4	Inferred from emissivity data in reference 1, figure 71

[a]Using semiempirical phase shifts.

TABLE II.- TABLE OF VALUES OF THE QUANTITIES OF L_o, Δ, $f(L/L_o) = I(400\ Å, 1130\ Å; L)/B(400\ Å, 1130\ Å)$ - Continued

$T = 8000^o$ K; $B(400\ Å, 1130\ Å, T) = 6.818\times10^{-1}$ watts cm^{-2} ster^{-1}									
ρ/ρ_o	10^{-6}	10^{-5}	10^{-4}	10^{-3}	10^{-2}	10^{-1}	10^{0}	10^{1}	10^{2}
L_o(cm)	8.53×10^{4}	6.88×10^{3}	6.35×10^{2}	6.26×10^{1}	6.72×10^{0}	9.19×10^{-1}	1.68×10^{-1}	3.26×10^{-2}	6.40×10^{-3}
Δ	11.332	11.330	11.328	11.328	11.342	11.460	12.271	14.798	17.525
$\alpha = L/L_o$	$f(\alpha)$	$f(\alpha)$	$f(\alpha)$	$f(\alpha)$	$f(\alpha)$	$f(\alpha)$	$f(\alpha)$	$f(\alpha)$	$f(\alpha)$
0.2	0.117	0.117	0.117	0.117	0.117	0.114	0.104	0.0843	0.0686
.4	.193	.193	.193	.193	.192	.186	.164	.126	.0961
.6	.252	.252	.253	.253	.251	.242	.213	.162	.121
.8	.301	.301	.301	.301	.299	.289	.255	.195	.145
1.0	.342	.342	.342	.342	.340	.329	.292	.225	.166
1.5	.424	.424	.424	.424	.422	.409	.367	.288	.215
2.0	.487	.488	.488	.488	.486	.472	.426	.340	.258
3.0	.587	.587	.588	.588	.585	.569	.518	.421	.327
4.0	.664	.665	.665	.665	.662	.645	.590	.485	.383
5.0	.727	.727	.728	.728	.724	.707	.649	.538	.429
7.0	.819	.819	.819	.819	.816	.800	.743	.625	.505
10.0	.902	.902	.903	.903	.900	.887	.839	.723	.594
$T = 9000^o$ K; $B(400\ Å, 1130\ Å, T) = 4.609\times10^{0}$ watts cm^{-2} ster^{-1}									
ρ/ρ_o	10^{-6}	10^{-5}	10^{-4}	10^{-3}	10^{-2}	10^{-1}	10^{0}	10^{1}	10^{2}
L_o(cm)	1.07×10^{5}	5.32×10^{3}	4.12×10^{2}	3.80×10^{1}	3.78×10^{0}	4.27×10^{-1}	6.65×10^{-2}	1.32×10^{-2}	2.80×10^{-3}
Δ	6.850	6.825	6.809	6.806	6.805	6.842	7.059	7.855	9.468
$\alpha = L/L_o$	$f(\alpha)$	$f(\alpha)$	$f(\alpha)$	$f(\alpha)$	$f(\alpha)$	$f(\alpha)$	$f(\alpha)$	$f(\alpha)$	$f(\alpha)$
0.2	0.126	0.127	0.127	0.127	0.127	0.126	0.123	0.114	0.0996
.4	.206	.207	.208	.208	.208	.206	.198	.177	.145
.6	.268	.270	.271	.271	.271	.269	.257	.227	.182
.8	.320	.322	.323	.323	.323	.320	.306	.269	.215
1.0	.363	.365	.367	.367	.367	.364	.347	.306	.246
1.5	.448	.451	.453	.453	.453	.449	.430	.383	.311
2.0	.513	.516	.518	.518	.519	.514	.494	.444	.365
3.0	.611	.614	.616	.617	.617	.612	.590	.536	.449
4.0	.685	.688	.690	.691	.691	.686	.663	.606	.514
5.0	.744	.747	.749	.749	.750	.745	.721	.662	.567
7.0	.830	.833	.835	.835	.835	.831	.809	.751	.651
10.0	.908	.910	.912	.912	.912	.908	.891	.841	.745

TABLE II.- TABLE OF VALUES OF THE QUANTITIES OF L_o, Δ, $f(L/L_o) = I(400\ Å, 1130\ Å; L)/B(400\ Å, 1130\ Å)$ - Continued

$T = 10{,}000^\circ$ K; $B(400\ Å, 1130\ Å, T) = 2.161\times10^{1}$ watts cm^{-2} ster^{-1}									
ρ/ρ_o	10^{-6}	10^{-5}	10^{-4}	10^{-3}	10^{-2}	10^{-1}	10^{0}	10^{1}	10^{2}
L_o(cm)	2.58×10^{5}	6.42×10^{3}	3.31×10^{2}	2.71×10^{1}	2.52×10^{0}	2.57×10^{-1}	3.32×10^{-2}	6.00×10^{-3}	1.32×10^{-3}
Δ	4.628	4.604	4.545	4.534	4.525	4.536	4.607	4.897	5.662
$\alpha = L/L_o$	$f(\alpha)$	$f(\alpha)$	$f(\alpha)$	$f(\alpha)$	$f(\alpha)$	$f(\alpha)$	$f(\alpha)$	$f(\alpha)$	$f(\alpha)$
0.2	0.135	0.135	0.136	0.136	0.136	0.136	0.135	0.132	0.123
.4	.218	.219	.221	.221	.222	.221	.219	.209	.187
.6	.282	.284	.287	.288	.288	.288	.283	.269	.236
.8	.335	.337	.341	.342	.343	.342	.337	.318	.278
1.0	.380	.382	.387	.388	.389	.388	.382	.360	.314
1.5	.467	.470	.476	.477	.478	.477	.470	.444	.390
2.0	.533	.536	.543	.544	.545	.544	.535	.508	.451
3.0	.630	.633	.640	.641	.642	.641	.632	.603	.542
4.0	.701	.704	.711	.712	.713	.712	.703	.673	.611
5.0	.756	.759	.766	.768	.769	.767	.759	.729	.665
7.0	.837	.840	.847	.848	.849	.848	.840	.811	.749
10.0	.911	.913	.918	.919	.920	.919	.913	.890	.835
$T = 11{,}000^\circ$ K; $B(400\ Å, 1130\ Å, T) = 7.754\times10^{1}$ watts cm^{-2} ster^{-1}									
ρ/ρ_o	10^{-6}	10^{-5}	10^{-4}	10^{-3}	10^{-2}	10^{-1}	10^{0}	10^{1}	10^{2}
L_o(cm)	8.29×10^{5}	1.13×10^{4}	3.37×10^{2}	2.20×10^{1}	1.87×10^{0}	1.84×10^{-1}	2.06×10^{-2}	3.25×10^{-3}	6.93×10^{-4}
Δ	3.368	3.323	3.276	3.255	3.240	3.241	3.264	3.394	3.761
$\alpha = L/L_o$	$f(\alpha)$	$f(\alpha)$	$f(\alpha)$	$f(\alpha)$	$f(\alpha)$	$f(\alpha)$	$f(\alpha)$	$f(\alpha)$	$f(\alpha)$
0.2	0.142	0.143	0.144	0.144	0.144	0.144	0.144	0.142	0.138
.4	.230	.232	.233	.234	.234	.234	.234	.229	.217
.6	.296	.299	.301	.303	.304	.303	.302	.295	.276
.8	.350	.354	.357	.359	.360	.360	.358	.348	.323
1.0	.396	.400	.404	.406	.408	.407	.405	.394	.364
1.5	.485	.490	.495	.498	.500	.500	.497	.482	.447
2.0	.552	.557	.563	.565	.567	.567	.564	.549	.511
3.0	.648	.653	.659	.662	.664	.664	.661	.644	.605
4.0	.716	.722	.728	.731	.733	.733	.729	.713	.673
5.0	.769	.774	.780	.783	.785	.785	.782	.766	.727
7.0	.845	.850	.856	.858	.860	.860	.857	.843	.806
10.0	.915	.919	.923	.925	.926	.926	.924	.913	.882

TABLE II.- TABLE OF VALUES OF THE QUANTITIES OF L_o, Δ, $f(L/L_o) = I(400\ Å, 1130\ Å; L)/B(400\ Å, 1130\ Å)$ - Continued

$T = 12{,}000^\circ$ K; $B(400\ Å, 1130\ Å, T) = 2.276\times10^{2}$ watts cm^{-2} ster^{-1}									
ρ/ρ_o	10^{-6}	10^{-5}	10^{-4}	10^{-3}	10^{-2}	10^{-1}	10^{0}	10^{1}	10^{2}
L_o(cm)	2.41×10^{6}	2.47×10^{4}	4.52×10^{2}	2.09×10^{1}	1.57×10^{0}	1.43×10^{-1}	1.51×10^{-2}	2.03×10^{-3}	4.05×10^{-4}
Δ	2.563	2.541	2.496	2.468	2.452	2.445	2.455	2.515	2.707
$\alpha = L/L_o$	$f(\alpha)$	$f(\alpha)$	$f(\alpha)$	$f(\alpha)$	$f(\alpha)$	$f(\alpha)$	$f(\alpha)$	$f(\alpha)$	$f(\alpha)$
0.2	0.149	0.149	0.150	0.150	0.150	0.150	0.150	0.149	0.147
.4	.242	.243	.245	.246	.246	.246	.246	.244	.237
.6	.311	.313	.315	.317	.318	.318	.318	.314	.303
.8	.367	.369	.372	.375	.376	.376	.376	.371	.356
1.0	.414	.416	.420	.423	.424	.425	.424	.418	.400
1.5	.504	.507	.513	.516	.518	.519	.518	.510	.488
2.0	.571	.574	.581	.584	.587	.588	.586	.578	.553
3.0	.667	.670	.676	.680	.682	.683	.682	.673	.648
4.0	.733	.736	.743	.747	.749	.750	.749	.740	.715
5.0	.784	.787	.793	.797	.799	.800	.799	.790	.766
7.0	.856	.859	.864	.868	.870	.870	.869	.862	.839
10.0	.921	.923	.927	.930	.931	.932	.931	.925	.908
$T = 13{,}000^\circ$ K; $B(400\ Å, 1130\ Å, T) = 5.719\times10^{2}$ watts cm^{-2} ster^{-1}									
ρ/ρ_o	10^{-6}	10^{-5}	10^{-4}	10^{-3}	10^{-2}	10^{-1}	10^{0}	10^{1}	10^{2}
L_o(cm)	6.10×10^{6}	6.31×10^{4}	8.30×10^{2}	2.38×10^{1}	1.41×10^{0}	1.20×10^{-1}	1.20×10^{-2}	1.42×10^{-3}	2.54×10^{-4}
Δ	2.033	2.011	1.967	1.961	1.930	1.921	1.925	1.952	2.054
$\alpha = L/L_o$	$f(\alpha)$	$f(\alpha)$	$f(\alpha)$	$f(\alpha)$	$f(\alpha)$	$f(\alpha)$	$f(\alpha)$	$f(\alpha)$	$f(\alpha)$
0.2	0.154	0.154	0.155	0.155	0.155	0.155	0.155	0.155	0.154
.4	.253	.253	.255	.255	.257	.257	.257	.256	.252
.6	.325	.326	.329	.329	.331	.332	.332	.330	.324
.8	.382	.384	.388	.388	.391	.392	.391	.389	.380
1.0	.430	.432	.437	.437	.440	.441	.441	.438	.428
1.5	.522	.524	.530	.531	.535	.537	.536	.532	.519
2.0	.589	.592	.599	.600	.604	.606	.605	.601	.586
3.0	.683	.686	.693	.694	.699	.701	.700	.696	.680
4.0	.748	.751	.758	.759	.764	.765	.765	.760	.745
5.0	.796	.800	.806	.807	.812	.813	.813	.808	.793
7.0	.865	.868	.873	.874	.878	.879	.879	.875	.862
10.0	.926	.928	.932	.933	.936	.937	.937	.934	.924

TABLE II.- TABLE OF VALUES OF THE QUANTITIES OF L_o, Δ, $f(L/L_o) = I(400\ \text{Å}, 1130\ \text{Å}; L)/B(400\ \text{Å}, 1130\ \text{Å})$ - Continued

$T = 14{,}000^\circ$ K; $B(400\ \text{Å}, 1130\ \text{Å}, T) = 1.271\times10^3$ watts cm^{-2} ster^{-1}									
ρ/ρ_o	10^{-6}	10^{-5}	10^{-4}	10^{-3}	10^{-2}	10^{-1}	10^{0}	10^{1}	10^{2}
L_o(cm)	1.40×10^{7}	1.42×10^{5}	1.65×10^{3}	3.10×10^{1}	1.40×10^{0}	1.05×10^{-1}	1.01×10^{-2}	1.10×10^{-3}	1.76×10^{-4}
Δ	1.655	1.625	1.636	1.609	1.569	1.557	1.558	1.570	1.627
$\alpha = L/L_o$	$f(\alpha)$	$f(\alpha)$	$f(\alpha)$	$f(\alpha)$	$f(\alpha)$	$f(\alpha)$	$f(\alpha)$	$f(\alpha)$	$f(\alpha)$
0.2	0.158	0.158	0.158	0.159	0.159	0.159	0.159	0.159	0.158
.4	.262	.263	.263	.264	.265	.266	.266	.265	.263
.6	.338	.340	.339	.341	.344	.344	.344	.343	.340
.8	.397	.400	.399	.401	.405	.406	.406	.405	.400
1.0	.446	.449	.448	.451	.455	.457	.457	.455	.449
1.5	.539	.543	.541	.545	.551	.553	.553	.551	.543
2.0	.606	.611	.609	.613	.620	.622	.622	.620	.611
3.0	.699	.704	.703	.707	.714	.716	.716	.714	.704
4.0	.762	.767	.766	.770	.777	.779	.779	.777	.767
5.0	.809	.814	.812	.816	.823	.825	.825	.823	.813
7.0	.874	.878	.876	.880	.886	.888	.888	.886	.878
10.0	.931	.934	.933	.936	.940	.941	.941	.940	.934
$T = 15{,}000^\circ$ K; $B(400\ \text{Å}, 1130\ \text{Å}, T) = 2.562\times10^3$ watts cm^{-2} ster^{-1}									
ρ/ρ_o	10^{-6}	10^{-5}	10^{-4}	10^{-3}	10^{-2}	10^{-1}	10^{0}	10^{1}	10^{2}
L_o(cm)	2.85×10^{7}	2.82×10^{5}	3.02×10^{3}	4.49×10^{1}	1.51×10^{0}	9.78×10^{-2}	8.77×10^{-3}	9.05×10^{-4}	1.31×10^{-4}
Δ	1.375	1.359	1.352	1.348	1.314	1.294	1.291	1.296	1.328
$\alpha = L/L_o$	$f(\alpha)$	$f(\alpha)$	$f(\alpha)$	$f(\alpha)$	$f(\alpha)$	$f(\alpha)$	$f(\alpha)$	$f(\alpha)$	$f(\alpha)$
0.2	0.161	0.161	0.162	0.162	0.162	0.162	0.162	0.162	0.162
.4	.270	.271	.271	.271	.273	.274	.274	.273	.272
.6	.349	.351	.351	.351	.354	.355	.356	.355	.353
.8	.411	.413	.413	.414	.417	.419	.419	.419	.416
1.0	.461	.463	.464	.464	.469	.471	.471	.471	.467
1.5	.555	.558	.559	.560	.565	.568	.569	.568	.563
2.0	.623	.626	.627	.628	.634	.637	.638	.637	.631
3.0	.715	.718	.719	.720	.727	.730	.731	.730	.724
4.0	.776	.779	.781	.781	.788	.791	.792	.791	.785
5.0	.821	.824	.825	.826	.832	.835	.836	.835	.829
7.0	.882	.885	.886	.886	.892	.895	.895	.895	.890
10.0	.936	.938	.939	.939	.943	.945	.946	.945	.941

TABLE II.- TABLE OF VALUES OF THE QUANTITIES OF L_o, Δ, $f(L/L_o)$ = I(400 Å, 1130 Å; L)/B(400 Å, 1130 Å) - Continued

T = 16,000° K; B(400 Å, 1130 Å, T) = 4.765×10^{3} watts cm^{-2} $ster^{-1}$									
ρ/ρ_o	10^{-6}	10^{-5}	10^{-4}	10^{-3}	10^{-2}	10^{-1}	10^{0}	10^{1}	10^{2}
L_o(cm)	5.70×10^{7}	5.39×10^{5}	5.61×10^{3}	7.03×10^{1}	1.71×10^{0}	9.54×10^{-2}	7.90×10^{-3}	7.82×10^{-4}	1.05×10^{-4}
Δ	1.162	1.153	1.152	1.142	1.118	1.099	1.091	1.093	1.113
$\alpha = L/L_o$	f(α)	f(α)	f(α)	f(α)	f(α)	f(α)	f(α)	f(α)	f(α)
0.2	0.164	0.164	0.164	0.164	0.165	0.165	0.165	0.165	0.165
.4	.277	.277	.277	.278	.279	.280	.280	.280	.279
.6	.360	.361	.361	.361	.363	.365	.365	.365	.364
.8	.424	.425	.425	.426	.429	.431	.431	.431	.429
1.0	.475	.477	.477	.478	.481	.484	.485	.484	.482
1.5	.571	.573	.573	.575	.579	.582	.583	.583	.580
2.0	.639	.640	.641	.643	.647	.651	.653	.652	.648
3.0	.730	.732	.732	.734	.739	.743	.744	.744	.740
4.0	.790	.791	.792	.794	.798	.802	.804	.803	.799
5.0	.833	.834	.835	.836	.841	.845	.846	.846	.842
7.0	.891	.892	.892	.894	.898	.901	.902	.902	.899
10.0	.941	.942	.942	.943	.946	.949	.950	.949	.947
T = 18,000° K; B(400 Å, 1130 Å, T) = 1.366×10^{4} watts cm^{-2} $ster^{-1}$									
ρ/ρ_o	10^{-6}	10^{-5}	10^{-4}	10^{-3}	10^{-2}	10^{-1}	10^{0}	10^{1}	10^{2}
L_o(cm)	1.83×10^{8}	1.64×10^{6}	1.67×10^{4}	1.76×10^{2}	2.77×10^{0}	1.01×10^{-1}	7.05×10^{-3}	6.42×10^{-4}	7.42×10^{-5}
Δ	0.916	0.862	0.864	0.855	0.847	0.826	0.816	0.814	0.819
$\alpha = L/L_o$	f(α)	f(α)	f(α)	f(α)	f(α)	f(α)	f(α)	f(α)	f(α)
0.2	0.167	0.168	0.168	0.168	0.168	0.168	0.169	0.169	0.169
.4	.286	.288	.288	.288	.289	.290	.290	.290	.290
.6	.373	.377	.377	.378	.379	.380	.381	.381	.381
.8	.440	.446	.446	.447	.448	.451	.452	.452	.451
1.0	.493	.501	.501	.502	.503	.506	.508	.508	.508
1.5	.590	.601	.600	.602	.604	.608	.610	.610	.609
2.0	.656	.668	.668	.670	.672	.677	.679	.680	.678
3.0	.744	.757	.757	.759	.761	.766	.768	.769	.768
4.0	.801	.814	.814	.816	.817	.822	.825	.825	.824
5.0	.842	.854	.853	.855	.857	.861	.864	.864	.863
7.0	.896	.906	.906	.907	.909	.913	.915	.915	.914
10.0	.943	.950	.950	.951	.952	.955	.956	.957	.956

TABLE II.- TABLE OF VALUES OF THE QUANTITIES OF L_o, Δ, $f(L/L_o) = I(400\ Å, 1130\ Å; L)/B(400\ Å, 1130\ Å)$ -. Continued

$T = 20{,}000^\circ K$; $B(400\ Å, 1130\ Å, T) = 3.240\times10^{4}$ watts cm^{-2} $ster^{-1}$									
ρ/ρ_o	10^{-6}	10^{-5}	10^{-4}	10^{-3}	10^{-2}	10^{-1}	10^{0}	10^{1}	10^{2}
L_o(cm)	7.73×10^{8}	4.56×10^{6}	4.17×10^{4}	4.21×10^{2}	5.15×10^{0}	1.25×10^{-1}	6.92×10^{-3}	5.72×10^{-4}	6.14×10^{-5}
Δ	0.846	0.710	0.674	0.671	0.664	0.652	0.639	0.635	0.637
$\alpha = L/L_o$	$f(\alpha)$	$f(\alpha)$	$f(\alpha)$	$f(\alpha)$	$f(\alpha)$	$f(\alpha)$	$f(\alpha)$	$f(\alpha)$	$f(\alpha)$
0.2	0.168	0.170	0.171	0.171	0.171	0.171	0.171	0.171	0.171
.4	.287	.294	.296	.296	.296	.297	.298	.298	.298
.6	.375	.387	.390	.390	.391	.392	.393	.394	.394
.8	.441	.459	.463	.464	.464	.466	.468	.468	.468
1.0	.493	.515	.521	.522	.523	.525	.527	.528	.527
1.5	.586	.616	.624	.625	.627	.629	.632	.633	.633
2.0	.648	.683	.693	.694	.695	.699	.702	.703	.703
3.0	.731	.770	.780	.781	.782	.786	.790	.791	.790
4.0	.787	.824	.833	.834	.836	.839	.843	.844	.843
5.0	.827	.861	.870	.871	.873	.876	.879	.880	.879
7.0	.881	.910	.918	.918	.920	.922	.925	.926	.925
10.0	.928	.951	.957	.957	.958	.960	.962	.963	.962
$T = 22{,}000^\circ K$; $B(400\ Å, 1130\ Å, T) = 6.692\times10^{4}$ watts cm^{-2} $ster^{-1}$									
ρ/ρ_o	10^{-6}	10^{-5}	10^{-4}	10^{-3}	10^{-2}	10^{-1}	10^{0}	10^{1}	10^{2}
L_o(cm)	4.85×10^{9}	1.35×10^{7}	9.27×10^{4}	9.06×10^{2}	1.01×10^{1}	1.74×10^{-1}	7.39×10^{-3}	5.51×10^{-4}	5.54×10^{-5}
Δ	0.794	0.633	0.559	0.543	0.540	0.531	0.519	0.513	0.514
$\alpha = L/L_o$	$f(\alpha)$	$f(\alpha)$	$f(\alpha)$	$f(\alpha)$	$f(\alpha)$	$f(\alpha)$	$f(\alpha)$	$f(\alpha)$	$f(\alpha)$
0.2	0.169	0.171	0.172	0.173	0.173	0.173	0.173	0.173	0.173
.4	.289	.297	.301	.302	.302	.302	.303	.303	.303
.6	.377	.392	.399	.400	.400	.401	.402	.403	.403
.8	.443	.465	.475	.477	.477	.478	.480	.481	.481
1.0	.494	.522	.535	.538	.538	.540	.542	.543	.543
1.5	.583	.622	.641	.645	.645	.648	.651	.652	.652
2.0	.642	.688	.710	.714	.715	.718	.721	.723	.723
3.0	.719	.771	.795	.800	.801	.804	.807	.809	.809
4.0	.772	.824	.846	.851	.852	.855	.858	.860	.860
5.0	.811	.860	.881	.885	.886	.889	.892	.893	.893
7.0	.865	.907	.925	.928	.929	.931	.934	.935	.935
10.0	.914	.947	.960	.963	.963	.965	.967	.968	.968

TABLE II.- TABLE OF VALUES OF THE QUANTITIES OF L_o, Δ, $f(L/L_o) = I(400\ \text{Å}, 1130\ \text{Å}; L)/B(400\ \text{Å}, 1130\ \text{Å})$ - Concluded

$T = 24{,}000^\circ$ K; $B(400\ \text{Å}, 1130\ \text{Å}, T) = 1.244\times10^5$ watts cm^{-2} $ster^{-1}$									
ρ/ρ_o	10^{-6}	10^{-5}	10^{-4}	10^{-3}	10^{-2}	10^{-1}	10^{0}	10^{1}	10^{2}
L_o(cm)	3.27×10^{10}	5.44×10^{7}	2.19×10^{5}	1.79×10^{3}	1.84×10^{1}	2.60×10^{-1}	8.42×10^{-3}	5.50×10^{-4}	5.22×10^{-5}
Δ	0.667	0.591	0.492	0.456	0.450	0.443	0.433	0.427	0.426
$\alpha = L/L_o$	$f(\alpha)$	$f(\alpha)$	$f(\alpha)$	$f(\alpha)$	$f(\alpha)$	$f(\alpha)$	$f(\alpha)$	$f(\alpha)$	$f(\alpha)$
0.2	0.171	0.172	0.173	0.174	0.174	0.174	0.174	0.174	0.174
.4	.295	.299	.304	.306	.306	.306	.307	.307	.307
.6	.387	.394	.404	.407	.408	.408	.409	.410	.410
.8	.457	.467	.481	.487	.487	.488	.490	.491	.491
1.0	.511	.525	.543	.550	.551	.552	.554	.555	.555
1.5	.604	.624	.650	.660	.662	.663	.666	.668	.668
2.0	.664	.688	.719	.731	.733	.735	.738	.740	.740
3.0	.740	.768	.803	.815	.817	.819	.823	.825	.826
4.0	.790	.818	.852	.864	.866	.868	.872	.874	.874
5.0	.827	.853	.885	.896	.898	.900	.903	.905	.905
7.0	.877	.900	.927	.936	.937	.939	.942	.943	.943
10.0	.922	.941	.961	.967	.968	.969	.971	.972	.972

$\Delta = 0.0$	
α	$1 - e^{-\alpha}$
0.2	0.18127
.4	.32968
.6	.45119
.8	.55067
1.0	.63212
1.5	.77687
2.0	.86466
3.0	.95021
4.0	.98168
5.0	.99326
7.0	.99909
10.0	.99995

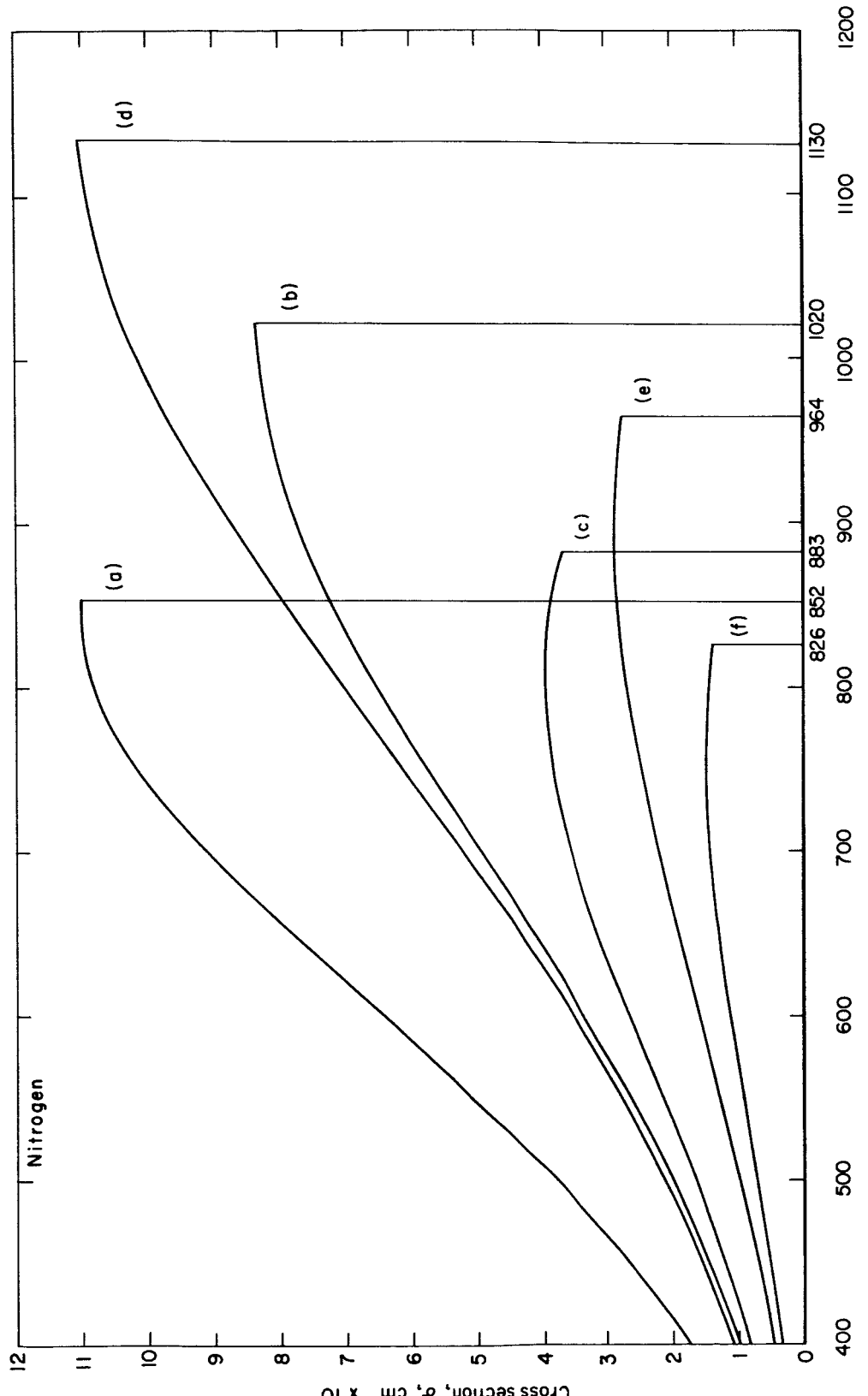

Figure 1.- Photoionization cross sections for nitrogen.

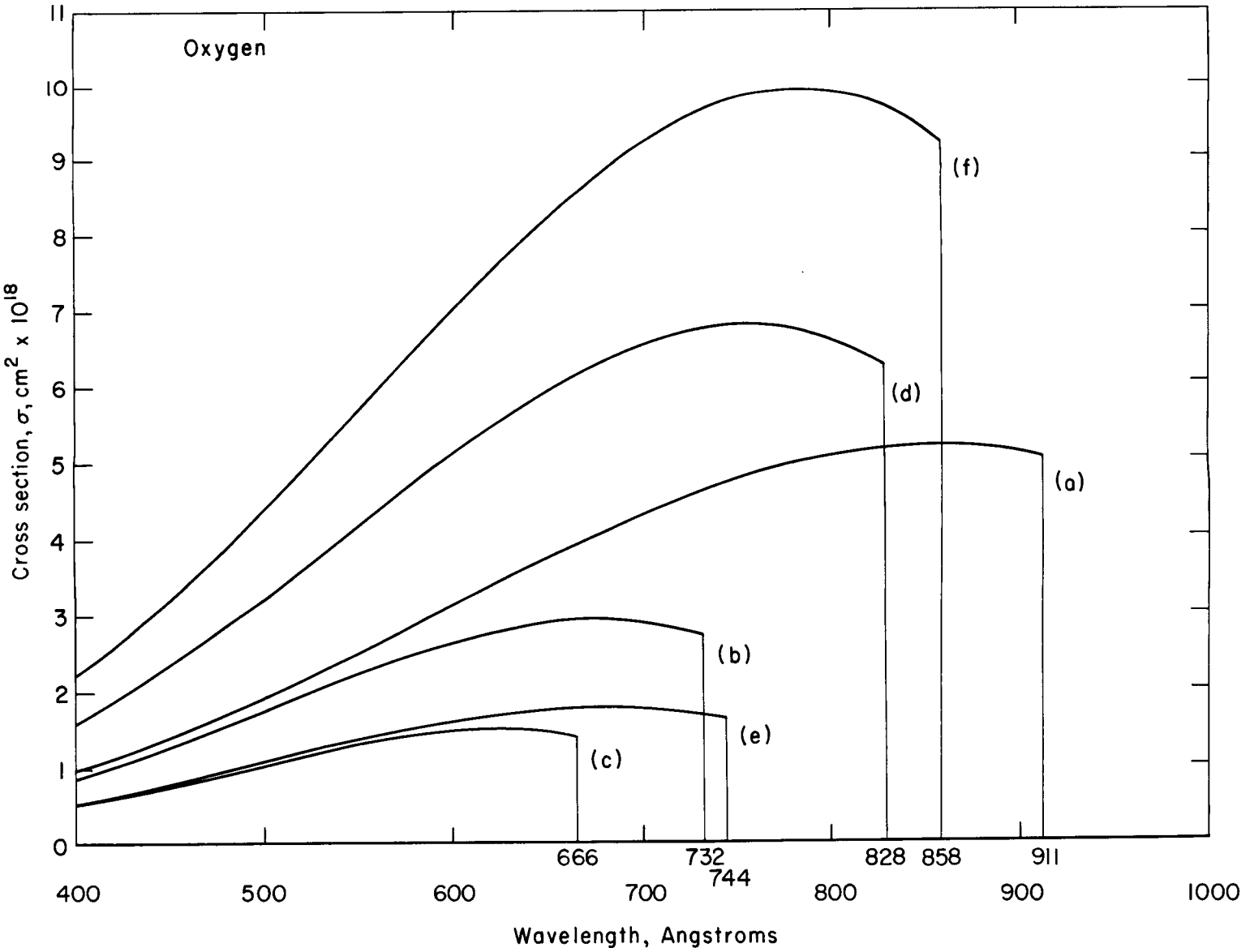

Figure 2.- Photoionization cross sections for oxygen.

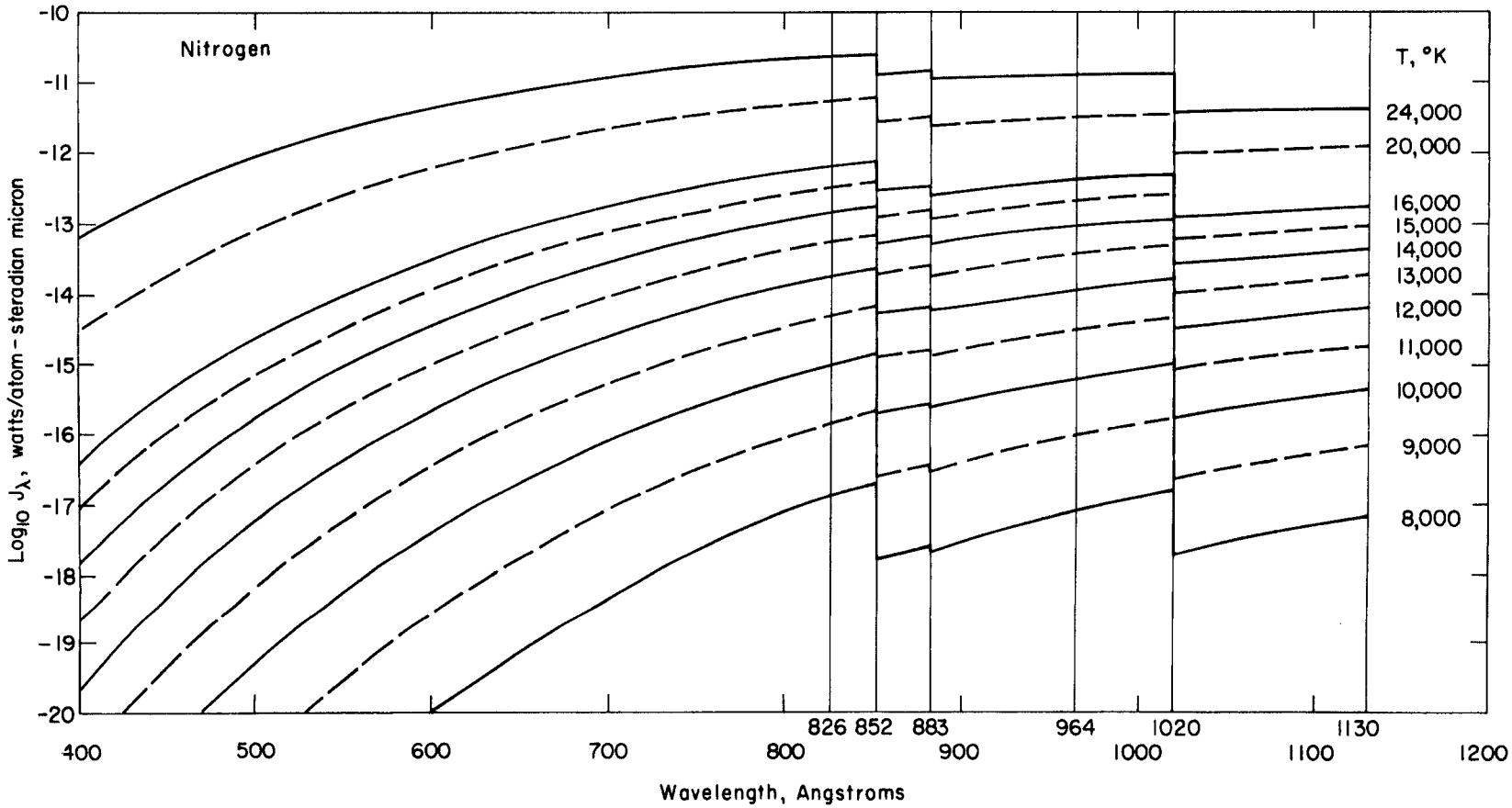

Figure 3.- Monochromatic emission coefficient for an average nitrogen atom.

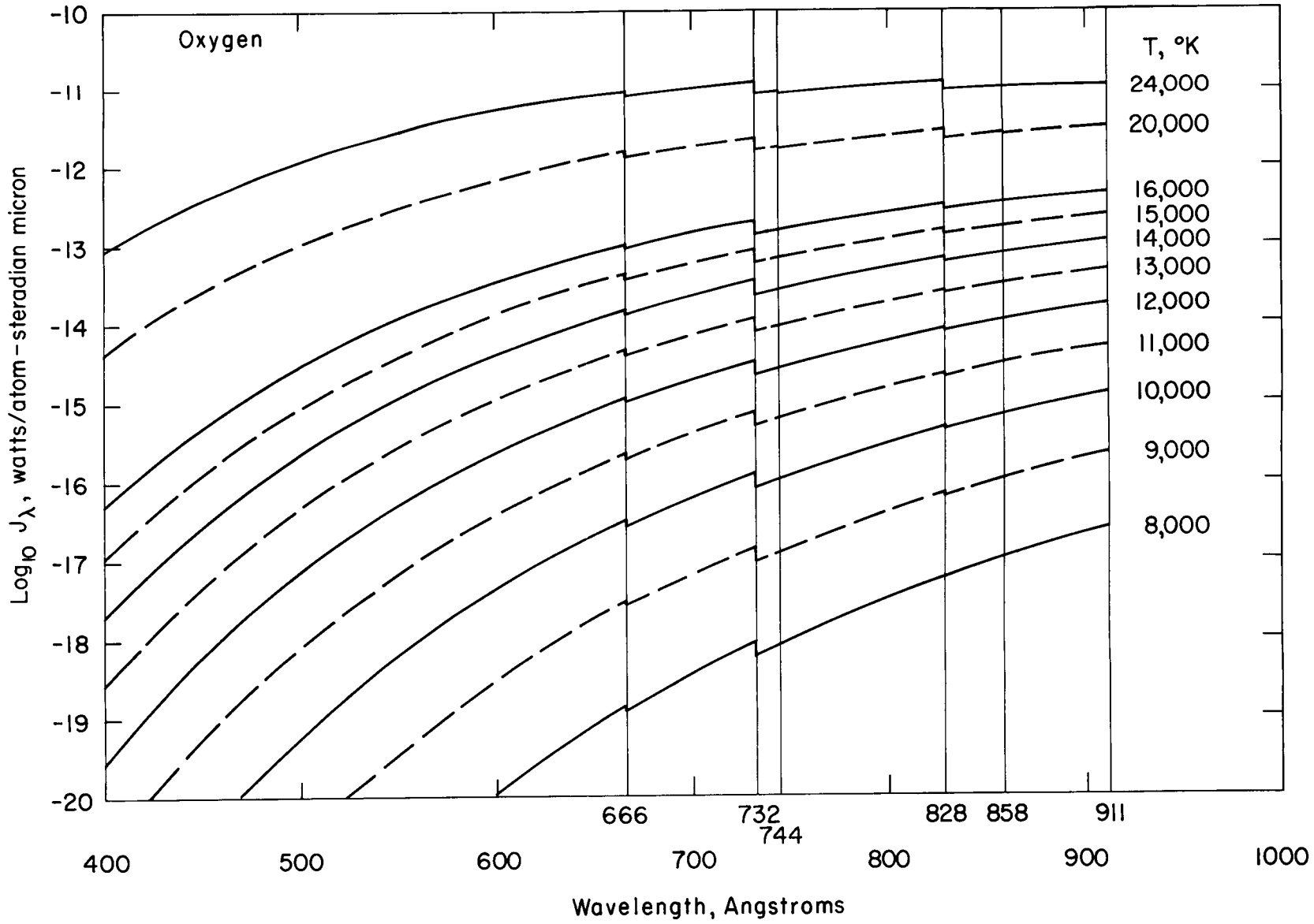

Figure 4.- Monochromatic emission coefficient for an average oxygen atom.

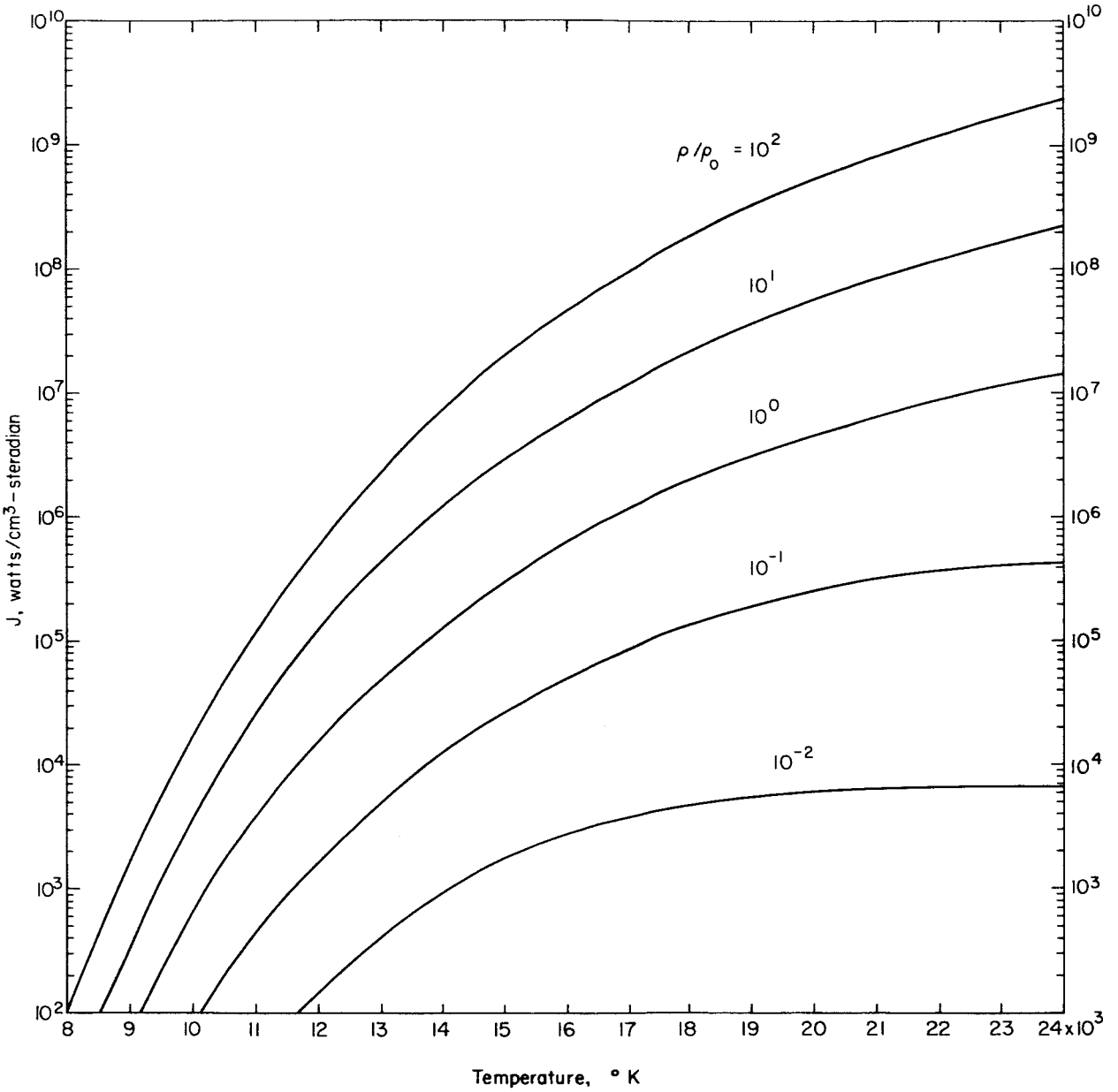

(a) $10^{-2} \leq \rho/\rho_o \leq 10^2$

Figure 5.- Integrated emission coefficient for air, J = J (400 Å, 1130 Å).

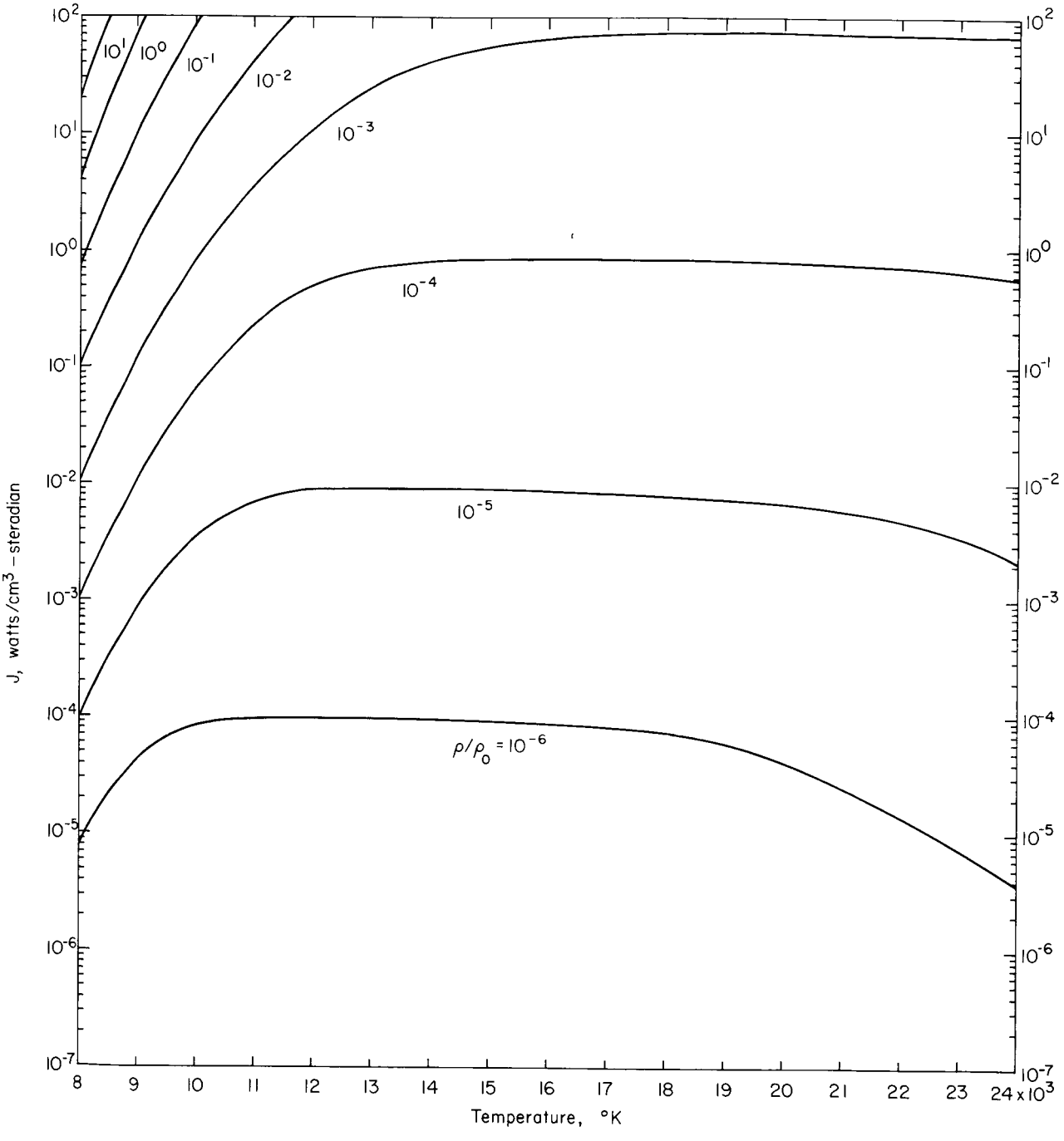

(b) $10^{-6} \leq \rho/\rho_0 \leq 10^{-3}$

Figure 5.- Concluded.

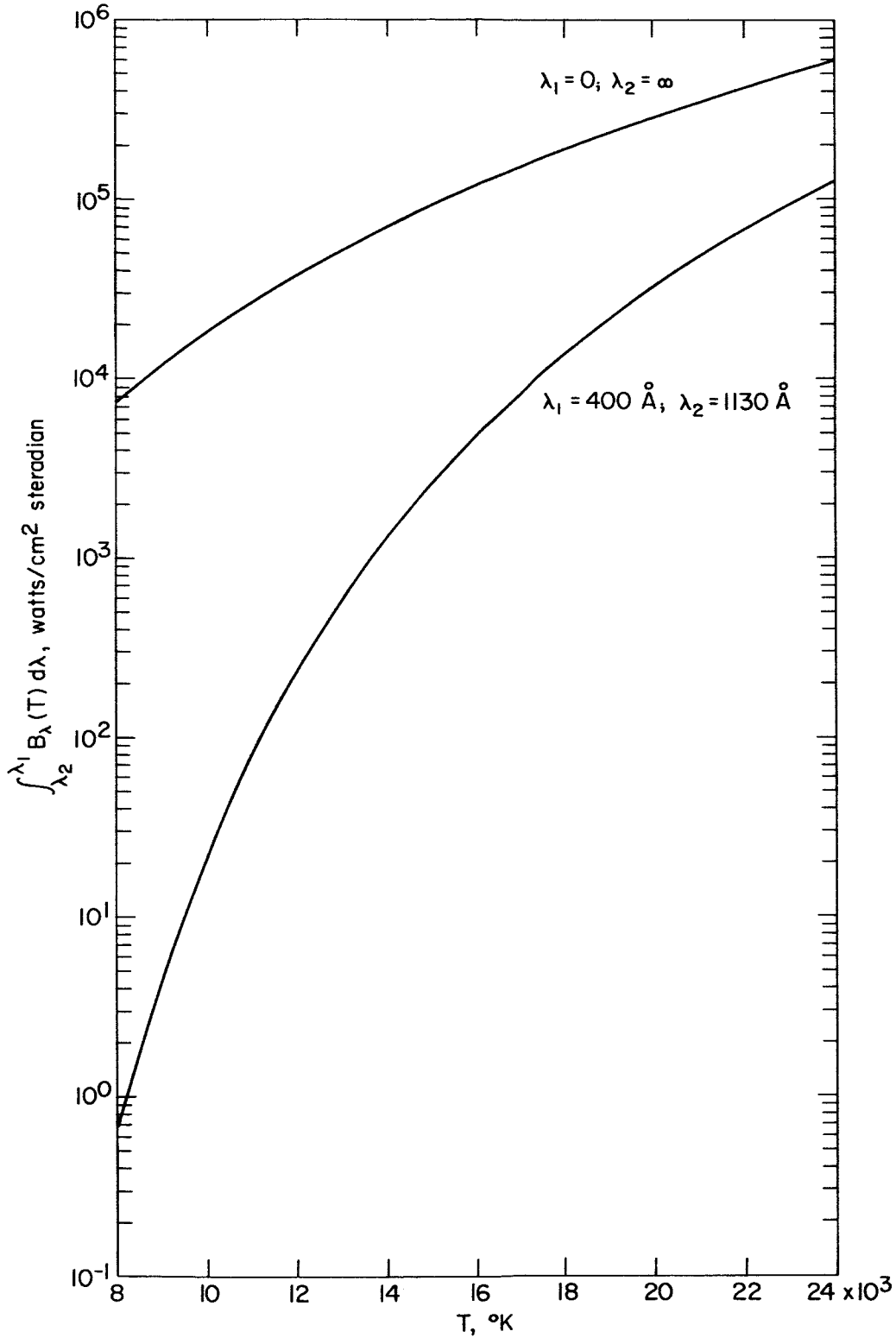

Figure 6.- Selected integrals for the Planck function.

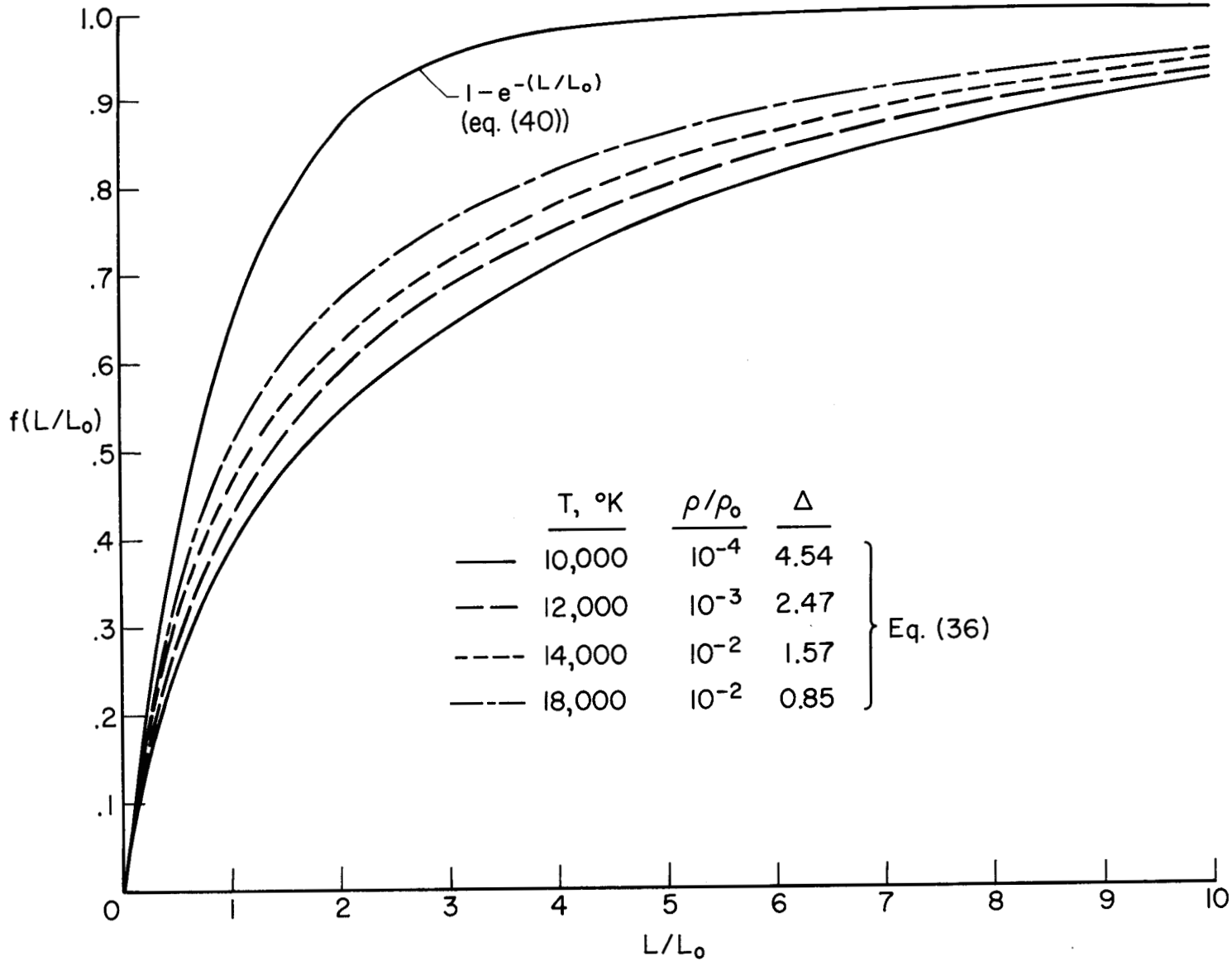

Figure 7.- Selected curves of $f(L/L_0) = I(400\ \text{Å}, 1130\ \text{Å}; L)/B(400\ \text{Å}, 1130\ \text{Å})$ as a function of L/L_0.

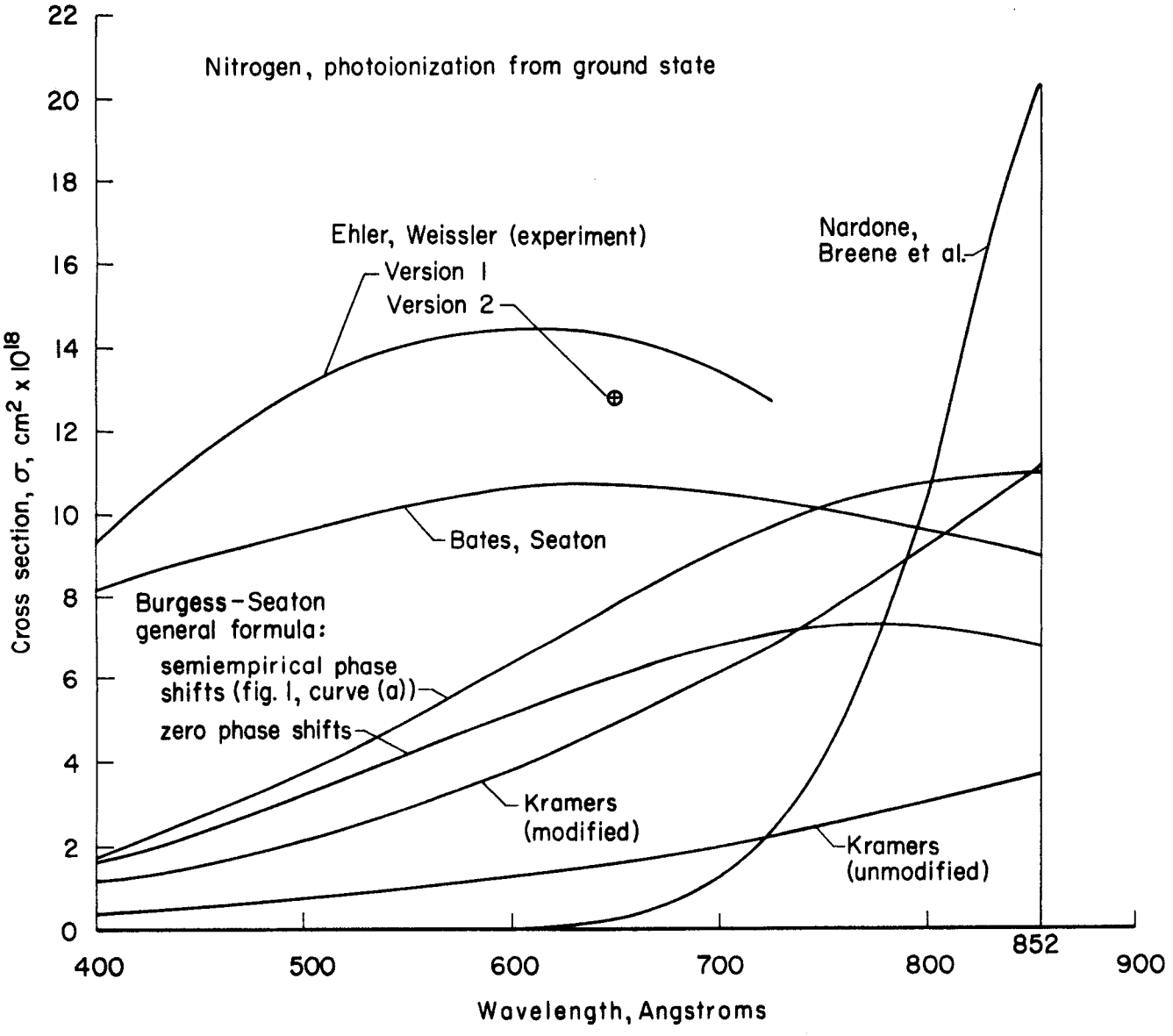

Figure 8.- Comparison of nitrogen ground state photoionization cross sections.

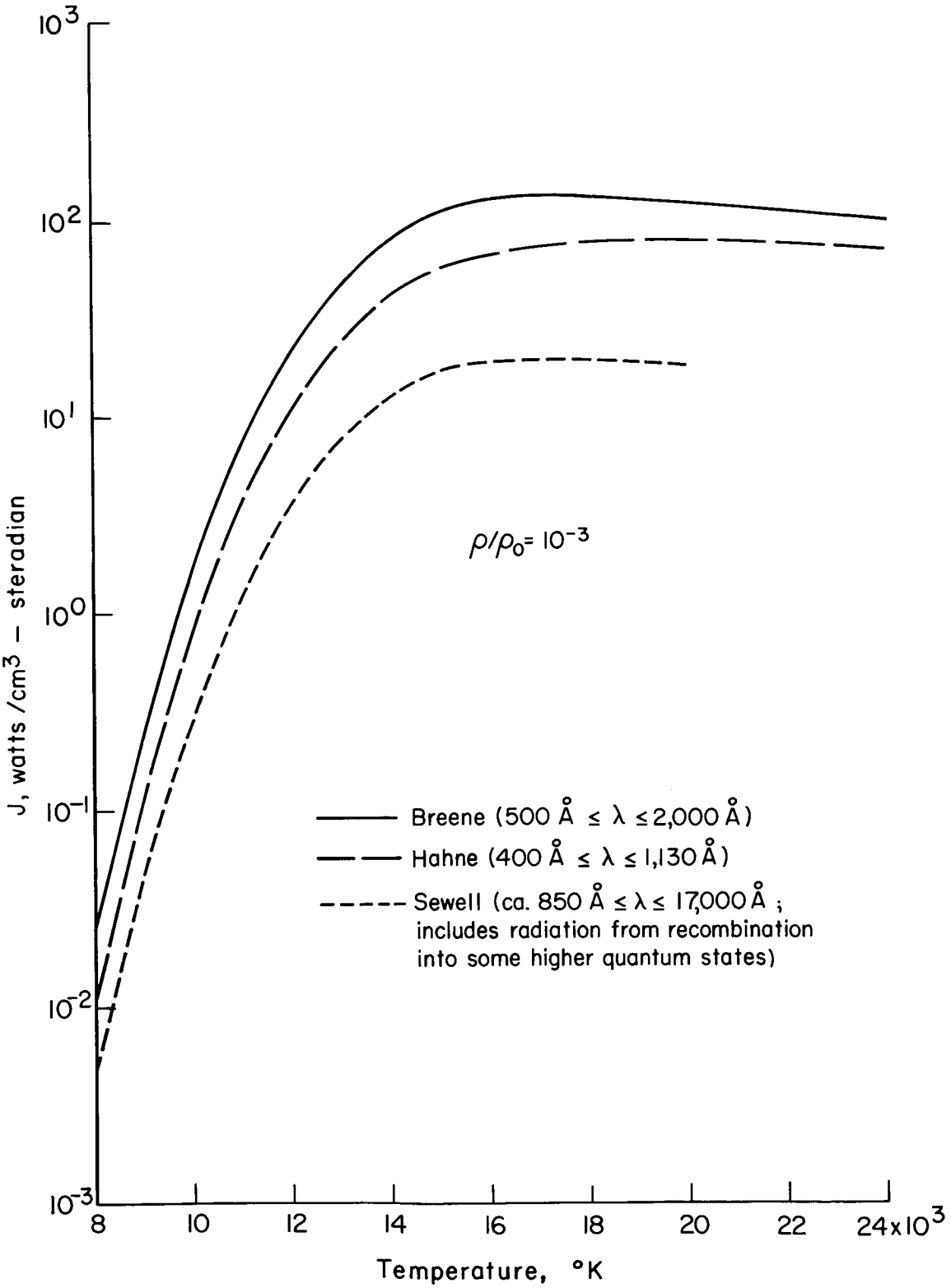

Figure 9.- Comparison of predictions of integrated emission coefficient for air.

NASA-Langley, 1965 A-992